Exploration of the *in-vivo* regulation of PMK-3 and MAK-2 after axotomy of *C. elegans* mechanosensory neuron

A Dissertation submitted by

Vibha Viswanath

to the

BRIC-National Brain Research Centre Gurgaon

in partial fulfillment of the requirements for the degree of

Master of Science in Neuroscience

June 2025

Exploration of the *in-vivo* regulation of PMK-3 and MAK-2 after axotomy of *C. elegans* mechanosensory neuron

A Dissertation submitted by

Vibha Viswanath

under the supervision of

Dr. Anindya Ghosh Roy

to the

BRIC-National Brain Research Centre Gurgaon

in partial fulfillment of the requirements for the degree of

Master of Science in Neuroscience

June 2025

ब्रिक – राष्ट्रीय मस्तिष्क अनुसंधान केंद्र
BRIC – National Brain Research Centre
(जैव प्रौद्योगिकी अनुसंधान एव नवाचार परिषद, भारत सरकार)
एन० एच०–08, मानेसर–122 052 (हरियाणा), भारत
(An Institute of the Biotechnology Research and Innovation Council, Govt. of India)
NH-08, Manesar - 122 052 (Haryana), INDIA

CERTIFICATE

This is to certify that the dissertation report entitled 'Exploration of the in-vivo regulation of PMK-3 and MAK-2 after axotomy of *C. elegans* mechanosensory neurons' is the result of work carried out by Vibha Viswanath at the National Brain Research Centre, Manesar, India, for partial fulfilment of requirements for the M.Sc. degree.

The work presented herein is original and has not been submitted previously for the award of any degree or diploma to National Brain Research Centre (Deemed to be University) or to any other University. This work is based on the guidelines of National Brain Research Centre (Deemed to be University) and is a record of the candidate's own efforts.

ANINDYA GHOSH ROY

(Supervisor's name and signature)

(Director, NBRC)

Place: Manesar

Date:

दूरभाष / Telephone : +91-124-2845200 फैक्स / Fax : +91-124-2338910
ई-मेल / E-mail : info.nbrc@nbrc.ac.in Website : www.nbrc.ac.in

Declaration by the Candidate

I, **Vibha Viswanath,** hereby declare that the work presented in the dissertation report entitled **"Exploration of the *in-vivo* regulation of PMK-3 and MAK-2 after axotomy of *C. elegans* mechanosensory neuron"** was carried out by me under the guidance of Dr. Anindya Ghosh Roy, Scientist-VI & Professor, Division of Cellular and Molecular Neuroscience, BRIC-National Brain Research Centre, Manesar, Haryana, India. I declare that no part of the thesis contains any plagiarized material. Any previously published or other material sourced from anywhere else has been appropriately attributed to the source. I also declare that no part of this thesis has been previously submitted for the award of any degree of diploma to BRIC-National Brain Research Centre or to any other university.

Place : Manesar

Date : 23rd June, 2021

Vibha Viswanath

M.Sc. Neuroscience (2024-2025)

Acknowledgement

I would like to extend my sincere gratitude to my supervisor, Dr. Anindya Ghosh Roy, Scientist-VI & Professor, BRIC-National Brain Research Centre for giving me the opportunity to work with him and his team for my M.Sc. Dissertation on the project titled "Exploration of the *in-vivo* regulation of PMK-3 and MAK-2 after axotomy of *C. elegans* mechanosensory neuron". This experience provided me an opportunity to think critically, function independently and develop understanding of the field, helping me build a platform for my future career goals. I would like to thank Dr. Sunanda Sharma for her constant guidance and support throughout my tenure. Extending my gratitude towards, Sukriti Aggarwal and Chakshu Mangal for their support. I would also like to thank the rest of the current and past lab members Dr. Sibaram Behera, Pallavi Singh, Dr. Swagatha Dey, Supraja, Mydthily Vasudevan, Aarya Patil, Dhyey, Ishanee, Dikshalee and Atiti for their guidance and company. Thanks, should also go to Mr. Sumit Mahapatra, and Mr. Prasenjit for their technical assistance in making NGM plates and stock solutions. I am particularly thankful to my friends and batch mates, Austin Varughese, Atharva Parolekar, Shashwati Tripathi, Vinitha Vinod, Dhrubajyoti Biswas for their constant support, presence and encouragement making my journey here at NBRC wholesome. Special thanks to my family and friends for their moral support. I am also thankful for all the non-academic staff of NBRC for making my stay comfortable. I am grateful to National Brain Research Center for giving me the opportunity to be a part of this Masters in Neuroscience Programme.

Abbreviations

MAP - Mitogen-activated protein

C.elegans - *Caenorhabditis elegans*

DLK - Dual leucine zipper kinase

CNS - Central nervous system

PNS - Peripheral nervous system

ALM (L/R) - Anterior Lateral Microtubule Cell (Left/Right)

PLM (L/R) - Posterior Lateral Microtubule Cell (Left/Right)

AVM- Anterior Ventral Microtubule Cell

PVM- Posterior Ventral Microtubule Cell

TRNs- Touch Receptor Neurons

DNA- Deoxyribonucleic Acid

NGM- Nematode Growth Media

GFP- Green Fluorescent Protein

TagBFP – Tag Blue Fluorescent Protein

TagRFP – Tag Red Fluorescent Protein

PCR- Polymerase Chain Reaction

DRG - Dorsal Root Ganglion

JNK - Jun N-terminal Kinase

LLPS – Liquid-liquid Phase Separation

FRAP - Fluorescent Recovery After Photo bleaching

FRET - Fluorescence Resonance Energy Transfer

IDR - Intrinsically Disordered Region

UTR – Un-Translated Region

DMSO - Dimethyl Sulfoxide

TMP - Trimethylpsoralen

Table of Contents

Abstract 8

1) Introduction 9

1.1)Regenerative capacity varies across different regions of the nervous system 9

1.2)DLK pathway crucial for axon regeneration 10

1.3)*Caenorhabditis elegans,* a robust model system to study axon regeneration 11

1.4) Biomolecular condensates facilitates spatial organization within the cell 12

1.5) DLK pathway kinases have liquid-like structural properties 13

1.6) DLK pathway kinases undergo LLPS-mediated biomolecular condensates 14

2) Aims and objectives 16

3) Materials and methods 17

3.1) Growth and maintenance of *C.elegans* 17

3.2) Generation of *C.elegans* males and setting up a genetic cross 17

3.3) Genotyping of loss of function mutants of *C.elegans* 17

3.4) Generation of transgenic C.elegans strains using Microinjection 18

3.5) Preparation of DNA constructs by molecular cloning 20

3.5.1) Primer design 21

3.5.2) Choice of DNA polymerase 21

3.5.3) Agarose Gel electrophoresis (AGE) 21

3.5.4) Dpn-I digestion 22

3.5.5) PCR/Gel purification - Column & Silica bead method 22

3.5.6) Cloner Enhancer treatment 24

3.5.7) In-Fusion cloning 24

3.5.8) Gateway cloning: LR recombination reaction 24

3.5.9) Bacterial Transformation - Chemical method 24

3.5.10) Colony PCR 25

3.5.11) Preparation of antibiotic resistance plates 25

3.5.12) Plasmid Isolation – MK kit column method 25

3.5.13) Restriction digestion 26

3.5.14) Preparation of Glycerol stocks 26

3.5.15) Analyzing the Sanger's sequencing results 26

3.6) Visualization of neurons in *C.elegans* 27

3.6.1) Phenotyping of the touch-receptor neuron circuit using Mec scoring sheet 27

3.6.2) Length measurements of the PLM posterior process using Epifluorescence microscopy 28

3.6.3) Laser-mediated Axotomy of PLM anterior process 28
3.6.4) Visualization of PLM cell body using Confocal microscopy 28
4) Results 30
4.1) Generation of transgenic strains expressing fluorescently tagged PMK-3 and MAK-2 30
4.2) Phenotypic characterization of the touch-neuronal circuit due to PMK-3 and MAK-2 overexpression 34
Figure 4.2: Morphological changes in the touch-receptor neuron circuit due to PMK-3 and MAK-2 overexpression 35
4.3) PMK-3 and MAK-2 co-expression does not cause puncta formation in the PLM cell body 36
4.4) Increase in MAK-2 overexpression does not cause puncta formation in the PLM cell body 36
Figure 4.4: *pmk-3[+]* and *mak-2[++]* co-expression does not cause puncta formation in the PLM cell body at L4 stage 37
4.5) PLM Axotomy at L4 stage induces PMK-3 and MAK-2 puncta formation 38
4.6) PMK-3 and MAK-2 puncta increases in size upon axotomy on day 1 and day 3 adults 40
4.7) Preparation of DNA constructs for negative control and overexpression in different tissue 43
5) Discussion 45
6) Future prospects 48
7) References 49
8) Appendix 51

List of figures

Figure 4.1: Generation of *C.elegans* strains overexpressing PMK-3 and MAK-2 33
Figure 4.2: Morphological changes in the touch-receptor neuron circuit due to PMK-3 and MAK-2 overexpression 35
Figure 4.3: *pmk-3[+]* and *mak-2[+]* co-expression does not cause puncta formation in the PLM cell body at L4 stage 36
Figure 4.4: *pmk-3[+]* and *mak-2[++]* co-expression does not cause puncta formation in the PLM cell body at L4 stage..... 37
Figure 4.5: Axotomy induced PMK-3 and MAK-2 puncta formation in L4 stage 39
Figure 4.6: PMK-3 and MAK-2 puncta size increases upon axotomy performed on day 1 and day 3 adults 42
Figure 4.7: Preparation of DNA constructs for *dlk-1* endogenous expression of *pmk-3* and negative control 44

Abstract

Axonal injury, often resulting from trauma can cause disruption in the neural circuits leading to functional deficit. While some organisms and neuronal cell types have the ability to regenerate and gain functional recovery, the mammalian central nervous system particularly lacks this capability. Hence, understanding the cellular and molecular mechanism by which certain neurons are able to cause a regeneration response can help us develop therapeutics. One of the key pathways, the DLK/p38 MAP kinase pathway, is evolutionarily conserved and is crucial for axon regeneration. A recent *in-vitro* study by Ray et al. 2024, suggests that PMK-3 and MAK-2, the downstream kinases of DLK-1, undergo liquid-liquid phase separation mediated biomolecular condensates to increase their bioavailability. We hypothesize that, the ability of these kinases to form condensates might pose as a cellular mechanism by which the DLK pathway aids axon regeneration. To investigate further *in-vivo*, we employed the touch-receptor neuron circuit of *C.elegans* as our model system. In this study, transgenic strains with fluorescently tagged PMK-3 and MAK-2 were generated and were used to study their ability to form puncta as a response to axotomy.

Graphical Abstract

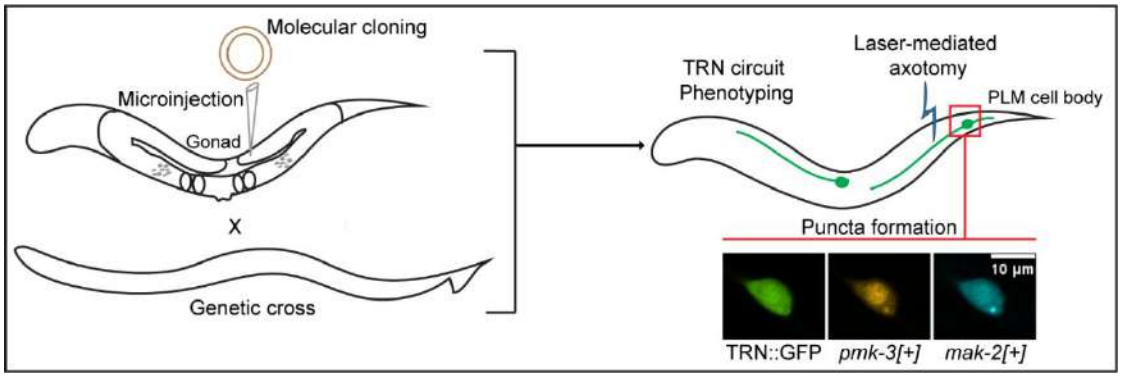

1) Introduction

Santiago Ramón y Cajal quoted that, “In adult centers the nerve paths are something fixed, ended, immutable. Everything may die, nothing may be regenerated. It is key for the science of the future to change, if possible, this decree.” Upon trauma, there is a loss of several kinds of tissue, but one of the kinds that do not have the ability to divide and replenish is the nervous system. Hence, it is very important for us to study the neuronal ability to regrow and attain functional recovery. This process is called neuronal regeneration. Over the century, there have been extensive research to uncover the mechanisms involved in neuronal regeneration failure in mature neurons. Several studies (He and Jin 2016) suggest that we can improve our understanding by investigating both intrinsic and extrinsic factors that influence the survival of the cell, which in turn affects its ability to regenerate. Extrinsic factors such as the extent of glial scarring, clearance of myelin debris, the integrity of extracellular matrix and distribution of growth factors become necessary to support the regrowth process. Whereas the intrinsic factors including the metabolic state of the cell, activation of pro-regenerative pathways and inhibition of apoptosis and regeneration inhibitory pathways become very crucial. Upon these favorable conditions, presence of guidance cues and growth factors would promote severed proximal neurite(s) to re-join the distal end. This regrowth of neurite would then be programmed to attain functional recovery.

1.1) Regenerative capacity varies across different regions of the nervous system

The nervous system is broadly divided into two subdivisions: 1) Central Nervous System (CNS) consisting of the brain and spinal cord, 2) Peripheral Nervous System (PNS) that innervates the entire body, connecting it to the CNS. There have been several unsuccessful attempts that have as yet progressed (Varadarajan, Hunyara et al. 2022) to regenerate the mammalian CNS axons. In contrast, the PNS axons have the ability to regenerate even in adulthood (Scheib and Hoke 2013). This could be because, they are surrounded by glial cells that undergo de-differentiation and further trans-differentiation enabling robust debris clearance. They also have cell-intrinsic responses to injury that promote axon regeneration compared to the CNS (Varadarajan, Hunyara et al. 2022). Hence, studying the cellular and molecular mechanisms that control PNS axon regeneration can help elucidate the neuron’s intrinsic ability to regenerate and promote the development of therapeutic interventions for neuro trauma.

1.2) DLK pathway crucial for axon regeneration

Dual leucine zipper kinase (DLK) signaling pathway is known to play a role in neuronal development, degeneration and regeneration as a response to injury. This cascade is organized as a series of mitogen associated protein kinase (MAPK), that includes MAP3K, MAP2K and MAPK, further activating numerous downstream targets such as transcriptional factors, membrane transporters, other protein kinases, and cytoskeletal elements. This pathway is responsible for neuronal migration and axonal growth during development (Tedeschi and Bradke 2013). Mutations in the *dlk* gene, protect several classes of neurons from undergoing degeneration and apoptosis. It also protects the distal axons from Wallerian degeneration caused due to injury (Tedeschi and Bradke 2013). Interestingly, the DLK pathway also promotes axon regeneration in different model systems (Chen and Chisholm 2011). In mouse DRG neurons, absence of the DLK gene leads to reduced neuronal regrowth, which was dependent on c-Jun. A Drosophila orthologue of DLK called Wallenda, is known to be upstream of the JNK and Fos cell-autonomous injury signaling cascade. DLK-1 in *C. elegans* was identified to be essential in axon regeneration of mechanosensory neurons. This promotes early steps of growth cone formation in injured axons. Upon injury, there is an elevation of Ca^{2+} levels, which activates DLK-1 (Figure 1.1). This further activates its downstream kinase cascade composed of MKK-4 (MAP2K), PMK-3 (MAPK) and MAK-2 (MAPKAP) followed by activation of a transcription factor cebp-1 promoting the regeneration response.

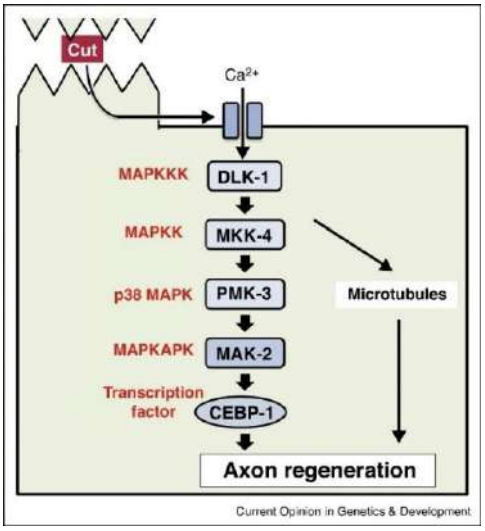

Figure 1.1: DLK pathway (Hisamoto and Matsumoto 2017)

Each of these kinases are known to be localized in various cellular compartments as mentioned in figure 1.2. DLK-1 is localized in the cytoplasm, axon, dendrite, synapse,

and cilia (Park, Glodowski et al. 2009); MKK-4 in cytoplasm, excluded from nucleus (Nakata, Abrams et al. 2005); PMK-3 in the cytoplasm and nucleus (Nakata, Abrams et al. 2005); MAK-2 in cytoplasm, nucleus, perikaryon, and synapse (Yan, Wu et al. 2009).

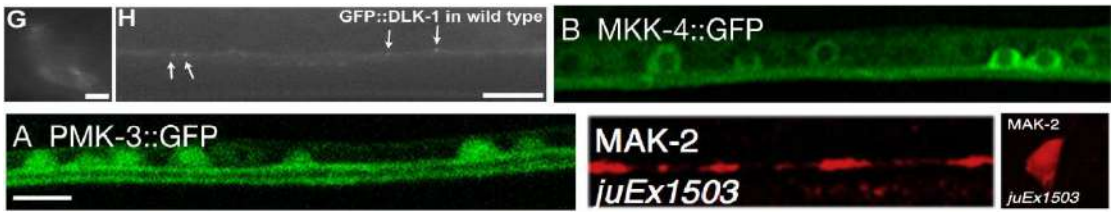

Figure 1.2: Cellular localization of DLK pathway kinases (Nakata, Abrams et al. 2005, Park, Glodowski et al. 2009, Yan, Wu et al. 2009)

1.3) *Caenorhabditis elegans,* a robust model system to study axon regeneration

C. elegans is a simple model organism with a short life span, the ability to produce large number of offsprings, and has a genome that is 40 to 70% conserved among evolutionarily higher animals. The nervous system of a *C. elegans* adult hermaphrodite consists of 302 neurons and its connectivity is mapped (Wormbook). The transparent body of the worm enables us to visualize fluorescently tagged molecular markers within the neuron in a live animal. The Touch Receptor Neuron (TRN) circuit is composed of six mechanosensory neurons (Figure 1.3) such as the Anterior Lateral Mechanosensory (ALM R/L), Posterior Lateral Mechanosensory (PLM R/L), Anterior Ventral Mechanosensory (AVM), and Posterior Ventral Mechanosensory (PVM). The PLM neuron consists of a cell body, a short posterior process and a long axon-like anterior process (Wormbook). Previous studies (He and Jin 2016) suggest that the anterior process of the PLM neuron serves as a good model system to study axon regeneration after axotomy.

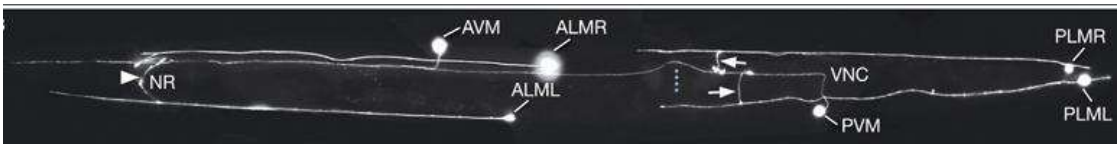

Figure 1.3: Mechanosensory touch-neuronal circuit in *C. elegans* (Wormbase)

Axotomy in *C. elegans* can be performed using femtosecond laser pulse (λ = 690-1020 nm) with a pulse energy range of 0.8 to 1.2 μJ (Rao, Kulkarni et al. 2008). The PLM axon present at the periphery of the worm's body makes it accessible to cause

optimum injury. The laser-mediated axotomy is performed approximately 50-60 µm away from the cell body with a cut site of 7 -10µm (Basu, Dey et al. 2017). This promotes growth cone initiation after 3 hours and growth cone formation at the tip of the severed axon after 6 hours post injury. Injury performed at the L4 larval stage of the worm yields robust regeneration after 24 to 48 hours (Basu, Dey et al. 2017).

C. elegans offers as a great model system to study the intrinsic mechanisms of axon regeneration at a single neuronal cell level *in-vivo*. Within the cell, a specific microenvironment needed for a physiological process to occur within the cytoplasm is attained by segregation using membrane bound and membrane-less organelles.

1.4) Biomolecular condensates facilitate spatial organization within the cell

Biomolecular condensates do not have any encapsulating membrane but exist stably within the cell. These are dynamical structures (Figure 1.4) that can be composed of various macromolecules such as proteins, nucleic acids, ions and co-factors among others (Wang, Zhang et al. 2021). This sort of compartmentalization can be achieved by the process of liquid-liquid phase separation (LLPS). Condensates are formed by three stages – 1) nucleation, the secondary or tertiary structure of the protein around which the remaining protein condensate is formed; 2) rearrangement, the molecules within the condensate are dynamic; 3) super saturation, growth of condensate size upon increase in molecules (Rostam, Ghosh et al. 2023). These processes are affected by the spontaneity of the biochemical process and critical concentration of the constituents. Several environmental factors such as pH, temperature and ionic strength become crucial for condensate formation. The nature of proteins that have a tendency to undergo LLPS are those that have low complexity regions and intrinsically disordered region characterized by the presence of amino acids that can undergo transient interactions such as π–π interactions, dipole–dipole interactions and ionic interactions (Wang, Zhang et al. 2021).

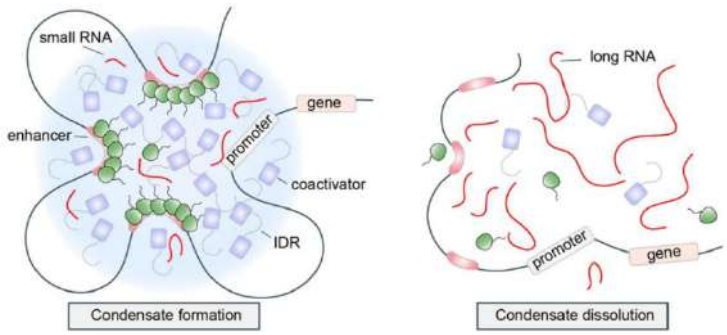

Figure 1.4: Pictorial representation of biomolecular condensate formation and dissolution (Wang, Zhang et al. 2021)

The LLPS based condensates are characterized by their circular structure. They are reversible and dynamic in nature. Several smaller condensates, to minimize energy, fuse to form bigger condensates. The presence of an IDR domain in at least some of the macromolecules is crucial for condensate formation.

In this field, there have been several techniques used (Ganser and Myong 2020) to elucidate the proposed theories of LLPS biomolecular condensates. One of the most common techniques used is Fluorescent Recovery After Photo-bleaching (FRAP) which can shed light on the molecular rearrangement of the molecules within the condensate (Andrusiak, Sharifnia et al. 2019). The fusion and fission properties of the fluorescently tagged macromolecules are also evaluated, as they are characteristic to condensate formation. Fluorescence Resonance Energy Transfer (FRET) can indicate the molecular interactions among the biomolecules. Optical tweezer assay provides information about the viscosity and surface tension of the condensate. Mass spectrometry can help identify the constituents of the condensates.

1.5) DLK pathway kinases have liquid-like structural properties

The DLK pathway kinases are structurally characterized and annotated by the Uniprot database (Apweiler, Bairoch et al. 2004). As mentioned in Table 1, all these kinases contain an intrinsically disordered region (IDR) responsible for undergoing condensate formation. This region is not a part of the protein kinase domain needed for phosphorylation activity. It is observed that the nature of amino acids lining the disordered region are acidic, basic, polar and low complexity residues.

Name of the protein	**Size of protein**	**Region description**	**Amino acid**
DLK-1	928 AA	Disordered region	1-72, 483-575,644-696, 802-845
		Protein kinase domain	135-377
		Leucine-zipper region	459-480
		SDGLSD hexa-peptide motif	874-879
		Interaction region across isoform a and c	605-814
MKK-4	363 AA	Disordered region	1 to 38
		Protein kinase domain	66-330
PMK-3	300 AA	Disordered region	1 to 90

		Protein kinase domain	114-419
MAK-2	366 AA	Disordered region	324-366
		Protein kinase domain	13-276
		Nuclear export signal	301-317
		Nuclear localization signal	330-353

Table 1:Structural composition of DLK pathway kinases

1.6) DLK pathway kinases undergo LLPS-mediated biomolecular condensates

A recent in-vitro study (Ray, Rao et al. 2024) propose that the downstream kinases of the DLK pathway, MAK-2 on its own can undergo biomolecular condensate formation while its upstream kinase PMK-3 undergoes aggregate formation. MAK-2 prevents this aggregation formation by undergoing LLPS mediated condensates. They also report that; the downstream kinase MAK-2 has the ability to phosphorylate its upstream kinase PMK-3 creating a feedback phosphorylation loop. This PMK-3 and MAK-2 condensate formation enables the bioavailability of the kinases suggesting their sustained activation during the signaling (Figure 1.5).

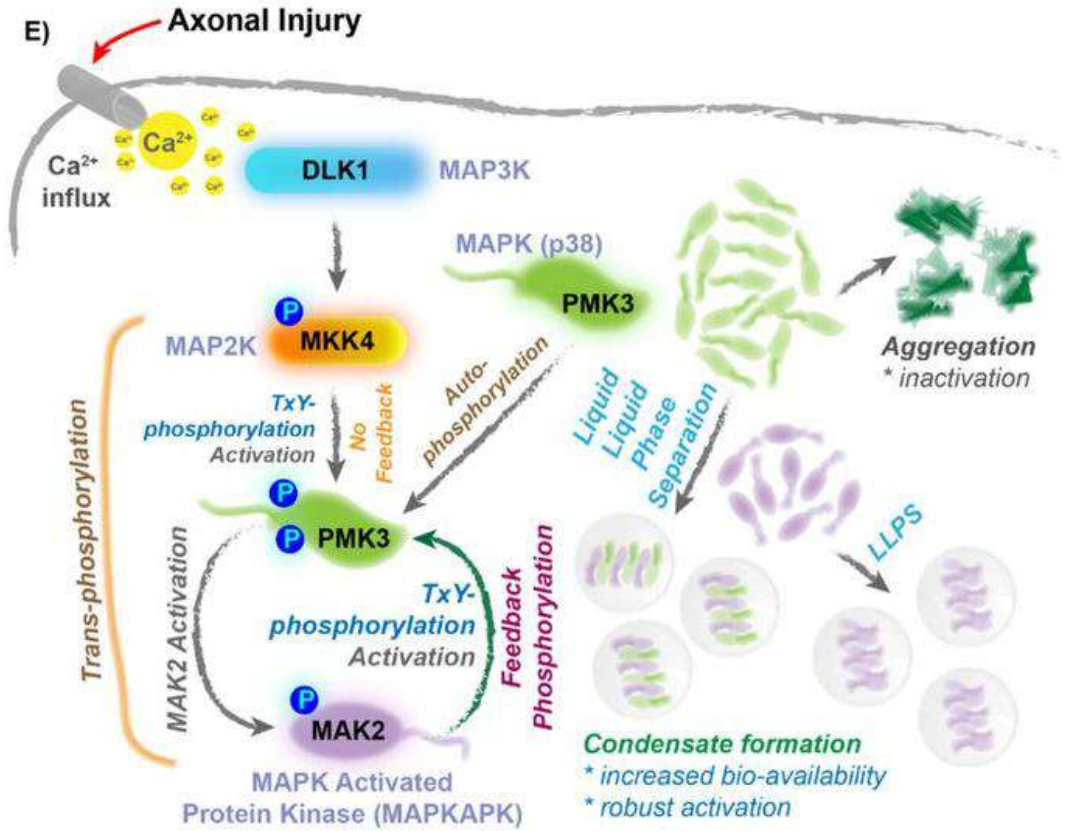

Figure 1.5: PMK-3 and MAK-2 undergo LLPS-mediated condensate formation in-vitro (Ray, Rao et al. 2024)

These *in-vitro* observations and theoretical evidences suggest that, the downstream kinases of the DLK pathway such as PMK-3 and MAK-2 can undergo LLPS driven condensate formation. To study this cellular phenomenon *in-vivo*, we employ the PLM mechanosensory neuron of *C. elegans* as a model system. Occurrence of this phenomena in-vivo can shed light onto the mechanistic aspect of DLK pathway driven axon regeneration.

2) Aims and objectives

We hypothesize, “PMK-3 and MAK-2 form liquid-liquid phase separation (LLPS) driven condensates to aid axon regeneration in *Caenorhabditis elegans*.”

The objectives of this study are as follows:

1) Preparation of DNA constructs by molecular cloning - PCR-8::*pmk-3*::TagRFP, *Pmec-4*::*pmk-3*::TagRFP, *Pmec-4*::TagBFP::*mak-2*, *Pmec-4*::TagBFP, *Pdlk-1*::*pmk-3*::TagRFP
2) Generation of transgenic *C.elegans* strains by
    a) Microinjection - TRN::TagBFP::*mak-2* (5ng) in TRN::GFP background
    b) Genetic cross - TRN::TagBFP::*mak-2* (5ng) in wild type background
3) Evaluation of PMK-3 and MAK-2 overexpression in the *C.elegans* touch-receptor neuron circuit by:
    a) Phenotypic observation of the mechanosensory touch-receptor neuron circuit by mec scoring
    b) Length measurements of the PLM mechanosensory neuron’s posterior process using Epifluorescence microscopy
    c) Observation of expression pattern of PMK-3 and MAK-2 in the PLM cell body using Confocal microscopy
4) To check if PMK-3 and MAK-2 co-overexpression causes puncta formation in L4 larval stage using Confocal microscopy
5) To check if PMK-3 and MAK-2 co-overexpression causes puncta formation in L4 larval stage using Confocal microscopy after laser-mediated axotomy
6) To check if PMK-3 and MAK-2 co-overexpression enhances puncta formation in day 1 and day 3 adults using Confocal microscopy post laser-mediated axotomy.

3) Materials and methods

3.1) Growth and maintenance of *C. elegans*

C. elegans was propagated on the standard Nematode Growth Medium (NGM) plate and an *E. coli* OP50 strain, an uracil auxotroph, was used as a bacterial food source. All strains were grown at 20ºC (Brenner 1974). Upon fungal or undesired bacterial growth on the NGM plate the worms were bleached. This was done by placing 15 to 20 gravid adult worms in a 1:1::NaOH: household bleach solution on a seeded NGM plate. The eggs containing a protective covering survive this process whilst the contaminants and adult worms die. The hatched eggs upon reaching L1 - L2 stage were transferred onto a fresh seeded NGM plate for further rearing.

3.2) Generation of *C. elegans* males and setting up a genetic cross

The males make up about 0.2% of the *C. elegans* population due to spontaneous disjunction of X-chromosome during meiosis (Wormbook). In the laboratory, males can be generated by providing heat shock at 32ºC to the L4 stage worms for 6 hours. This increase in temperature increases the probability of mis-segregation of the X-chromosome during germ cell meiosis (Wormbook). After the heat-shock, the worms were grown at 20ºC. In the F1 generation, about 2 to 5% of the population was composed of the male progeny. Upon setting up a cross with 12 males: 3 hermaphrodites in the ratio of 4:1 on a small bed seeded plate, the next generation had about 50% male progeny. This can also be used as a confirmation to determine the success of the genetic cross.

3.3) Genotyping of loss of function mutants of *C. elegans*

The genotype of the *C. elegans* mutant strain was determined by the following steps:

a) Preparation of lysis buffer and solution:

The lysis buffer for each reaction consisted of 2$\mu\ell$ of 10X homemade PCR buffer, 2$\mu\ell$ 25mM $MgCl_2$ and nuclease free water was used to make up the volume for a 20$\mu\ell$ reaction. A lysis solution was prepared by mixing lysis buffer with commercial Proteinase K in the ratio 9:1.

b) Lysis of worms:

15 to 20 gravid adults of the strain of interest were transferred into the lysis solution and were incubated at 60ºC for 1 hour for lysis and 65ºC for 15 minutes for heat inactivation of the proteinase.

c) Genotyping PCR:

10$\mu\ell$ of the PCR reaction was setup using the Emerald green premix protocol with 2$\mu\ell$ of the genomic lysates. The genotyping external forward primers (EFP) and external reverse primers (ERP) were designed outside and that of the internal forward primer (IFP) was designed inside the deletion region. Rationale behind this was that, the band obtained with the EFP+ERP for the mutant strain would be smaller than that of wild type while there won't be any band obtained with the IFP+ERP for the mutant strain (due to the deletion) against obtaining a band for the wild type strain.

3.4) Generation of transgenic *C. elegans* strains using Microinjection (Mello, Kramer et al. 1991)

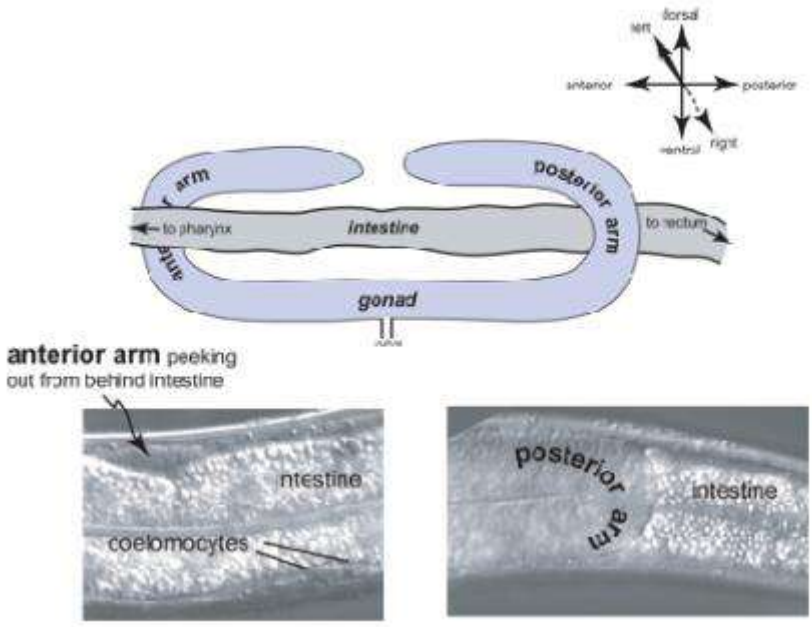

Figure 2.1: Microinjection performed in the early adult *C. elegans* gonad consists of anterior and posterior arm (Wormbook)

a) Preparation of agarose pads

3% agarose was prepared using 1X M9 buffer. Agarose beds were prepared by adding a drop onto a 22mm coverslip and placing another coverslip perpendicular to it. These were kept for air drying overnight followed by at 65ºC for 1 hour. The top coverslip was removed and the ones with the agarose beds were stored for further use.

b) Preparation of mouth pipette

A mouth pipette was made by attaching a grip (to hold the capillary) and a 200$\mu\ell$-pipette tip on either ends of a rubber tube.

c) Preparation of the injection mix:

The injection mix consisted of 2.5ng of *Pmyo2*::mCherry (co-injection marker), 5ng of *Pmec-4*::TagBFP::*mak-2* (desired plasmid) and 120ng of pBSK (buffer plasmid).

d) Preparation of injection needles

Glass capillaries were pulled to obtain the desired nature of the injectable tip using a stutter instrument. These needles were filled with an injection mix using another capillary and placed in an inclined manner to allow gravity to descend the injection mix to the tip of the needle.

e) Preparation of the mount and breaking the injection needle:

A thicker glass capillary was pulled over the flame to obtain a tapered end. A mount was prepared by sticking the tapered end onto a coverslip using halocarbon oil. The injection needle was attached to the holder on the scope. Using the micromanipulator, the needle was focused at the same plane as the prepared mount at 40X magnification and was placed perpendicular to it. Gently, the injection needle was hit against the mount to break the tip large enough to provide continuous flow of the DNA mixture.

f) Mounting the worm for microinjection:

On the agarose pad, a drop of halocarbon oil was placed and a worm at early adult stage was placed in it. Upon immobilization, the worm and the severed tip of the needle were focused at the same plane at 40X magnification. The needle was inserted into the worm gonad on either the anterior or the posterior side (transparent region) and two pulses of DNA mixture were injected into each worm.

g) Rescue of the injected worm:

Each worm was rescued by adding 1X M9 buffer and transferring them onto a seeded NGM plate separately using a mouth pipette. All plates were grown at 20ºC.

h) Selection of F1 progeny:

All the F1 progeny were checked for the presence of co-injection marker, being so, they were copied to new seeded NGM plates for further preparation.

i) Calculation of transmission efficiency:

The transmission efficiency was calculated to measure the amount of propagation of the extrachromosomal array to the subsequent generation. A single L4 staged worm from the F1 lines containing the co-injection marker was transferred onto a new seeded

plate. After 3 days, the transmission efficiency was calculated by the (number of worms having the co-injection marker) / (Total number of worms in the plate) * 100.

Plates having a transmission efficiency of greater than 70% are considered as high transmission lines and are used for experimental purposes.

3.5) Preparation of DNA constructs by molecular cloning

The clone of interest was designed by combining the DNA sequences of individual components on the ape software and the type of cloning procedures suitable was determined (Table 2). PCR was performed to obtain amplicons of individual components. Further, the vector backbone and insert amplicons were treated and processed by either of the following method:

a) Dpn-I restriction enzyme to break down the initial template. The amplicons were then purified using PCR purification or Gel extraction. The latter was used when the PCR product had non-specific band(s) that were not able to be removed by different amplification conditions. If the obtained amplicon was a single band with high DNA concentration, the former type of purification step was used.
b) If the PCR product yielded a single band with high concentration, they were treated with Cloner Enhancer (Takara).

All the components were then ligated the procedures of Infusion cloning or LR recombination. The ligated product was then transformed into chemical competent bacterial cells. Colony PCR was performed on the obtained colonies to screen for desired clones. Plasmid was isolated from the colonies showing positive results. On these plasmid(s), restriction digestion was performed causing single, double and triple cuts. The clones with positive digestion results were outsourced for Sanger sequencing and microinjected into the worm to create transgenic strains. The details of the molecular cloning protocol are mentioned in appendix, Table 1 to 5.

Clone	**Vector backbone**	**Insert**	**Type of cloning**
pNBRGWY188_PCR-8::*pmk-3*::TagRFP	PCR-8::*ptrn-1*::TagRFP sans *ptrn-1*	*pmk-3*	Infusion
pNBRGWY189_Pmec-4::*pmk-3*::TagRFP	*pmec-4* destination vector	*pmk-3*::TagRFP	Gateway

pNBR78_*pmec-4*::TagBFP::*mak-2*	*pmec-4*::mscarlet sans mscarlet	TagBFP, *mak-2*	Infusion
pNBR79_*pmec-4*::TagBFP	*pmec-4*::TagBFP::*mak-2* sans *mak-2*	N/A	Site-directed insertion - Infusion
pNBR80_*pdlk-1*::*pmk-3*::TagRFP	*pmec-4*::*pmk-3*::TagRFP sans p*mec-4*	*pdlk-1*	Infusion

Table 2: Strategy used to design the DNA constructs

3.5.1) Primer design

All PCR and genotyping primers designed (using ApE software) were of length ranging between 20-25 mer and the infusion primers (designed using Takara primer design tool) of 40-45 mer (with complementary overhangs) length. The GC% were maintained under 55%. The difference in melting temperature of forward and reverse primers was less than 5ºC. The primers were designed to avoid the formation of secondary structures, homo and heterodimers by maintaining the ΔG value lesser than -9kcal.

3.5.2) Choice of DNA polymerase

The following DNA polymerase/Premix were used for amplifications concerning molecular cloning and genotyping. The choice of this polymerase for the reaction depended on the size of the expected amplicon, the purpose of amplification, fidelity, low error rate, speed of the reaction and obtaining maximum yield. The PCR reaction components and conditions were followed as per the respective company's protocol and certain necessary changes were made. The details of all these reactions are mentioned in Appendix (Table 1).

3.5.3) Agarose Gel electrophoresis (AGE)

The DNA samples of sizes greater and lesser than 3kb were resolved using 0.8% and 1% agarose gels respectively. 1X TAE buffer was used to cast the gel and as a running buffer. EtBr was used as a DNA stain while 1X home-made gel loading dye mixed with the sample was used to track the DNA on the gel. Standard 1kb and 100bp ladders were used as a reference to compare band sizes. The DNA bands were resolved under a constant voltage of 80V or 130V and were visualized under a UV illuminator.

3.5.4) Dpn-I digestion

The PCR amplified products were treated with Dpn-1 restriction enzyme to digest the initial template plasmid at its methylated sites. This procedure was helpful to eliminate the template plasmid; on the off chance it would interfere with the cloning reaction itself and further contribute towards forming abundant negative colonies during screening. The entire quantity of PCR product in the presence of rcutsmart buffer was treated with 20 units of Dpn-I digestion for 3 hours at 37℃.

3.5.5) PCR/Gel purification - Column & Silica bead method

It can be performed using: a column method, consisting of a silica membrane or the silica bead method consisting of suspended silica beads with a coating (providing a positive charge) enabling the DNA (negatively charged) to bind. For the gel purification method, agarose gel containing the DNA was melted to mix and for PCR purification, the PCR product was directly mixed with the binding buffer. In the presence of chaotropic salts (pH ~ 5 to 6), the DNA was bound to the silica membrane/silica beads. The contaminants were removed by washing with an ethanolic wash buffer. Finally, the DNA was eluted with nuclease free water.

a) Column method: Macherey- Nagel kit

- For gel extraction of DNA, the agarose gel was exposed to UV for a minimum time and the desired bands were cut using a clean scalpel and transferred to a pre-weighed tube. The weight of the gel was measured and for each 100 mg of agarose gel (0.6%), 200 µl of buffer NTI (binding buffer) was added. The samples were incubated at 50ºC for 5 minutes with frequent mixing to dissolve the agarose completely.
- For PCR purification, for every 100μl of PCR product, 200μl of buffer NTI was added.

Subsequent steps were common for both PCR and gel purification.

- 700μl of DNA sample was added and bound to the clean-up silica column, incubated for 5 minutes for the binding, followed by centrifugation for 2 minutes at 11000g. The flow-through collected in the collection tube was discarded.
- 700μl of buffer NT3 (wash buffer) was added to the column and was spun for 2 minutes at 11,000g. The flow-through collected in the collection tube was discarded. This step was repeated twice.

- An empty spin was conducted for 2 minutes at 11,000g to remove any residual wash buffer. The column was air dried for 3 minutes.
- The membrane was transferred to a new collection tube. The DNA was eluted in 30-50μl of nuclease-free water by adding it into the column and incubating it for 5 minutes. The tube was spun for 2 minutes at 11,000g. Two elution were done to get maximum yield.
- The concentration of the DNA obtained was measured using Nanodrop (Spectrophotometer) and the integrity of the desired DNA fragment was verified by resolving the sample by AGE.

b) Silica bead method: Thermo-Scientific kit

- During gel extraction, the DNA fragment from the gel is excised using a clean scalpel and weighed. Binding buffer was added to the tube in the 3:1 ratio of volume of the Binding buffer: weight of the agarose gel. The gel mixture was incubated at 55℃ for up to 5 minutes until it dissolved completely.
- During PCR purification, the binding buffer: PCR product was mixed in the ratio of 3:1.

Subsequent steps were common for both PCR and gel purification.

- 5μl of resuspended silica powder was added to the DNA-binding buffer mixture (<2.5ug). The mixture was incubated at 55℃ for 5 minutes. The mixture was regularly mixed to ensure homogenous silica suspension.
- The silica powder-DNA complex was spun for 2 minutes at 11,000g to form a pellet and the supernatant was discarded.
- The pellet was resuspended in 500μl of ice-cold wash buffer and centrifuged for 2 minutes at 11,000g. The supernatant was discarded. This process was repeated 2 times. The pellet was air-dried for 5 to 7 minutes to remove ethanolic contamination.
- The pellet was resuspended in 30μl of nuclease-free water and incubated at room temperature for 5 minutes. This was centrifuged for 2 minutes at 11,000g. The supernatant containing the DNA was transferred to another tube and the elution step was repeated.
- The DNA concentration was measured using Nanodrop and the integrity of the DNA was evaluated by resolving the sample by AGE.

3.5.6) Cloner Enhancer treatment

5μl of PCR product with good concentration and single band was treated with 2μl of cloner enhancer (by Takara) and was incubated in the thermocycler at 37℃ for 15 minutes and 80℃ for 15 minutes heat inactivation. The product obtained was further used for Infusion reaction.

3.5.7) In-Fusion cloning

For a 5μl infusion reaction, 1μl of the 5X In-Fusion HD enzyme premix was added along with the linearized vector and inserts in the molar ratio of 2:1 (Details present in appendix Table 2). The volume of the reaction mixture was made up using nuclease-free water. This reaction mixture was incubated at 50℃ for 15 minutes. The reaction mixture was then transformed into chemical competent cells for further process or stored at - 20℃ until further use.

3.5.8) Gateway cloning: LR recombination reaction

The reaction mixture consisted of 0.5 μl of 1X TE buffer, LR clonase, 5X LR clonase buffer and 37.5ng of entry clone (PCR-8::*pmk-3*::TagRFP) and 37.5 ng of destination vector (*Pmec-4* Gateway). This reaction mixture was incubated at 25℃ for 1 hour in the thermocycler. Further, 0.5 μl of Proteinase K was added and incubated at 37℃ for 30 minutes. This was then transformed into chemical competent cells for further process.

3.5.9) Bacterial Transformation - Chemical method

1.5μl of each ligated product was transformed into 50μl of stellar competent cells (transformation efficiency - 3 x 10^8) using chemical method of bacterial transformation. Both mixed together were incubated on ice for 30 minutes. Heat shock was provided to the mixture at 42℃ for 45 seconds. Immediately, the tubes were incubated on ice for 5 minutes. 500μl SOC media was added to the culture and incubated at the 37℃-shaker incubator for 1 hour for recovery of bacteria. The culture was plated onto its corresponding antibiotic resistance LB plate and was kept at 37℃ for 8 to 12 hours. The obtained colonies were restreaked and a colony lysate was tested for the desired colony.

3.5.10) Colony PCR

The colony lysate was prepared by dissolving a small inoculum of the colony of interest in 10μl of 1X TE buffer and incubating it at 65℃. For each clone in preparation, 16 to 48 colonies were screened. Each colony PCR reaction mixture was composed of 2μl of colony lysate, Emerald PCR premix complemented with 10μM of suitable forward and reverse primers made up to 10μl using nuclease free water. Detailed PCR conditions used for each colony PCR is mentioned in appendix ().

3.5.11) Preparation of antibiotic resistance plates

Antibiotic stock of 100mM for all antibiotics were prepared. The LB agar was prepared and autoclaved. Carbenicillin, Spectinomycin and Chloramphenicol were added to LB agar in their working concentrations of 100 µM, 50 µM and 100 µM respectively and poured into 90mm petri plates. The solidified agar plates were stored at 4℃.

3.5.12) Plasmid Isolation – MK kit column method

The pelleted bacteria were resuspended by the resuspension buffer and the cells are broken down by the alkaline lysis method. The neutralization buffer was used to precipitate proteins, genomic DNA and cell debris. The supernatant containing the DNA was bound to the silica membrane. Any contaminants present was washed off by the wash buffer and the DNA was eluted in nuclease free water.

- A single transformed bacterial colony was inoculated into 15ml of LB broth and incubated at 37℃ with constant shaking for 15 hours.
- The bacterial culture was then pelleted by centrifuging it at 4000rpm for 20 minutes.
- The bacteria were resuspended in 250μl of resuspension buffer.
- 250μl of lysis buffer was added and mixed gently. 300μl of neutralization buffer was added and centrifuged at 11,000g for 2 minutes.
- The supernatant was transferred onto the nucleo-spin column for binding of DNA onto the silica membrane. It was centrifuged at 11,000g for 2 minutes. The elute was discarded.
- 700μl of wash buffer was added onto the column and was centrifuged at 11,000g for 2 minutes. This step was repeated twice. An empty spin was done to remove any residual wash buffer.

- The DNA was eluted in nuclease free water by its incubation on the column for 5 minutes and centrifuged at 11,000g for 2 minutes.
- The concentration of the obtained DNA was measured using Nanodrop (Spectrophotometer).

3.5.13) Restriction digestion

Positive clones selected by colony PCR were confirmed by digesting them using restriction enzymes. The DNA sample in the presence of rcutsmart buffer was treated with 5 units of high fidelity (HF) restriction enzymes for 30 minutes while non-HF enzymes were treated for 3 hours at 37℃. The digested sample was resolved using AGE.

3.5.14) Preparation of Glycerol stocks

Bacteria transformed with the plasmid of interest were inoculated in LB broth and incubated in the shaker at 37℃ for 12 hours. 50% Glycerol was made using Autoclaved Milli Q water. The bacterial culture and 50% glycerol were mixed in the 1: 1 ratio in a cryo-vial (on ice) and was stored at -80℃.

3.5.15) Analyzing the Sanger sequencing results

The specific promoter, gene and reporter regions were sequenced by the Sanger's method from the Genomic facility of Advanced technology platform center, Regional Center for Biotechnology, Faridabad, India.

a) Primer designing:

The primers for sequencing were designed 50 bp upstream of the region to be sequenced. The primers generated followed the same rules as previously mentioned in this section.

b) Sample preparation:

10mM of primers and 100 to 200 ng/μl of plasmid with 260/280 and 260/230 ratio ranging from 1.7 to 2 and 1.4 to 2 respectively.

c) Analysis of results: The ApE software was used for analysis;

- The quality of the sequencing results was assessed for single nucleotide peaks of higher amplitude and width for confidence and accuracy of its base calling.

- The initial 50 to 90 bp and end of the sequencing data containing overlapping peaks with low confidence were not considered for analysis.
- The base callings of the confidence regions were sequence aligned with the original ape file sequence to locate for discrepancy and marked. In case so, the sequencing procedure was repeated to know if it is a sequencing error or a generated mutation.

3.6) Visualization of neurons in *C. elegans*

The transgenic *C. elegans* lines were visualized using fluorescence microscope. On a glass slide, a 5 to 7.5% agarose bed was made using 1X M9 buffer. 2 μl of 10mM Levamisole, a drug used to immobilize worms was added. The worms were transferred onto the slide and mounted with a coverslip. The position of the worms was marked and was visualized at different magnifications.

3.6.1) Phenotyping of the touch-receptor neuron circuit using Mec scoring sheet

The touch-receptor neuron circuit of *C. elegans* was visualized and evaluated for any morphological changes caused due to overexpression of PMK-3 and MAK-2. All the strains were observed at the L4 stage and compared the neuronal phenotype with the wild type strain using 40X magnification (NA=0.75) of Leica upright fluorescent microscope. Any additional morphological changes were noted on the Mec scoring sheet that has a diagrammatic representation of the circuit. All the PMK-3 and MAK-2 overexpression strains were compared against wild type. All the observations were plotted as a contingency plot and Fisher's exact statistical test was employed to compare across each group.

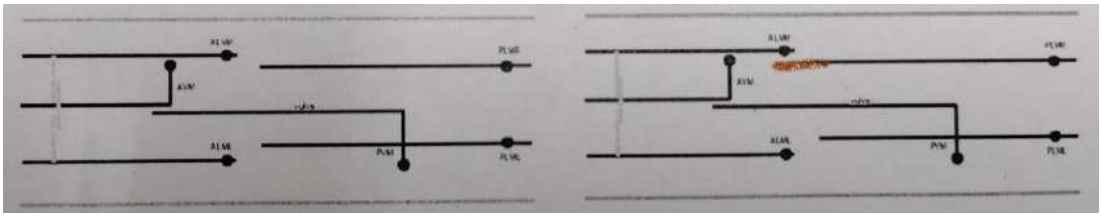

Figure 2.2: Mec scoring sheet marked with overgrowth of PLM anterior process (right) in MAK-2 overexpression compared against wild type (left)

The lengths of the anterior and posterior process of the PLM neuron were evaluated by a self-created matrix. The PLM posterior process was visually evaluated by the number of PLM cell bodies needed to cover the entire length. Up to 6 PLM cell body length of the PLM posterior process was observed in the wild type strain (Normal),

while in certain overexpression strains, they were longer (very long). The PLM anterior process was evaluated by its length crossing the ALM cell body (overgrowth) or if it ends earlier, creating a gap between the ALM cell body and the end of PLM anterior process (Gap). The ALM posterior process was evaluated by its presence or absence.

3.6.2) Length measurements of the PLM posterior process using Epifluorescence microscopy

The tail region consisting of the PLM neuron of the TRN::TagBFP::*mak-2 [+]* line-2 in TRN::GFP background and wild type strain was imaged at 100ms exposure using Nikon Ti-2 microscope at 40X magnification (oil objective, NA = 1). Image analysis was performed using ImageJ software. The acquired images were Z-stacked at maximum intensity projection and the length measurement of the PLM posterior process was done for both strains and noted. The Mann-Whitney U test statistical test was performed to compare both the groups.

3.6.3) Laser-mediated Axotomy of PLM anterior process

The worms of all the life stages were immobilized using 2 μl of 10mM Levamisole on a 7.5% agarose bed. The worm was observed at 100X (oil objective, NA= 1.5) and the tail region was focused. Axotomy was to be performed using a femtosecond multiphoton laser setup (Basu, Dey et al. 2017). This was performed on the PLM anterior process about 50 to 65 µm distance away from the cell body. Two laser shots were given to aid 10 µm cut. The injured worms were rescued using 1X M9 buffer and transferred to a seeded plate and kept at 20 ℃. For different experiments, the worms were further imaged 15 minutes and 3 hours post injury.

3.6.4) Visualization of PLM cell body using Confocal microscopy

The PLM cell body was visualized using Nikon AXR confocal point-scanning microscope at 100X magnification (NA= 1.45) and 3X zoom. The pinhole size used was 1AU, the dwell time while acquiring each image was 39.2 seconds per frame using Galvano scanner. The optical resolution obtained was 0.23µm. All the transgenic strains were excited with 405nm, 488nm and 561nm to visualize blue, green and red fluorescence reporters. Because of presence of multiple fluorescence reporters within the same strain, there are chances of bleed through across channels. To cater to this, several parameters such as the emission wavelength, laser intensities and gain were manipulated and standardized. The detector emission range was set to 429-474nm, 532-549nm, 596-628nm to capture TagBFP, GFP and TagRFP signal. The scanning

was also performed sequentially by using the minimal crosstalk feature. The laser parameters and gain used to visualize TagBFP was 15% and 30, GFP was 0.3% and 30, TagRFP was 35% and 30. The worm's morphology was observed using Differential interference contrast microscopy. The worms of L4, day 1 and day 3 stage of all strains were immobilized on a 7.5% agarose bed and visualized. Z-stacks were captured for each PLM cell body. The imaging parameters to visualize PLM cell body for all strains at all life stages were kept constant.

All the acquired images were analyzed by individual channels. All the z-stacks were evaluated by visual inspection for the slices containing. These were stitched together to form a montage. The brightness/contrast adjustments were done to aid better visualization of the puncta. The number of puncta per cell body was calculated for all experimental conditions when the puncta was visualized in the same spatial location of the cell in both red and blue channel across different z-slices indicating the PMK-3 and MAK-2 both form the puncta. These puncta were plotted as a mean box plot.

4) Results

DLK/p38 MAP kinase pathway, evolutionarily conserved is known to play a crucial role in axon regeneration. A recent *in-vitro* study (Ray, Rao et al. 2024) suggests that the downstream kinase of this pathway, PMK-3 on its own has a tendency to form aggregates but when it interacts with MAK-2, together forms biomolecular condensates. They further suggest that this kind of interactions among the said proteins may increase their bioavailability, crucial for carrying out their function. We aim to investigate if PMK-3 and MAK-2 can form biomolecular condensates *in-vivo*. For this study, we employ the use of the PLM touch-receptor neuron (TRN) of *C. elegans* as a model system to investigate if overexpression of PMK-3 and MAK-2 causes puncta formation in-vivo and if they play a role in axon regeneration.

4.1) Generation of transgenic strains expressing fluorescently tagged PMK-3 and MAK-2

To study this phenomenon *in-vivo* at a single cell level, we used the touch-neuronal circuit of *C. elegans* as our model system. This circuit has 6 mechanosensory neurons, namely - 2 ALM, 2 PLM,1 AVM and 1 PVM neurons (Figure 4.1 D). The anterior process of the PLM neuron is axon-like in nature and they have been extensively used in the field to study axonal regeneration (Basu, Dey et al. 2017). For this reason, *pmk-3* and *mak-2* were expressed under the touch-receptor neuron (TRN) circuit specific *mec-4* promoter (Figure 4.1A-C). TagRFP and TagBFP were chosen as reporters for PMK-3 and MAK-2 respectively to determine its localization within the cell. For protein aggregation and condensate formation-based studies, it was important to choose reporters that inherently have the least ability to form oligomers within the cellular environment. TagBFP remains as a monomer whereas TagRFP can form a weak dimer. The pka values (affects the fluorescence intensity) of each of them are 2.7 and 3.8 respectively, which is much lower than cellular pH, making them suitable reporters for this study (Lambert 2019). Unc-54 is a 3' UTR that is commonly used in the field (Boulin, Etchberger et al. 2006) which helps in efficient processing of transcripts and maintaining its stability.

These constructs were introduced into *C.elegans* gonad using Microinjection (Mello, Kramer et al. 1991). Multiple copies of this DNA mixture together form an extrachromosomal array, whose replication is independent of that of the host genome and they do not follow Mendelian genetics form of inheritance. As the oocytes mature, the gonadal nuclei along with some portion of the cytoplasm containing the injected

DNA array was encapsulated. The transformed F1 progeny were selected by the presence of co-injection marker expressed in the pharyngeal muscles and were single-selfed. After successful injection I obtained 2 transgenic lines of TRN::TagBFP::*mak-2* expressed in TRN::GFP background and their transmission efficiency was calculated to be 84% and 79%. To visualize *pmk-3*::TagRFP, *mak-2*::TagBFP and the diffusible GFP reporter in the PLM neuronal cell body, the imaging parameters were standardized. The expression pattern of TagBFP::*mak-2* in the PLM neuron was observed to be as in Figure 4.1F. *pmk-3*::TagRFP expression and 1:1 co-overexpression of *pmk-3*::TagRFP and TagBFP::*mak-2* (strain generation credit: Chakshu Mangal) was observed as mentioned in figure 4.1 E and G.

While imaging green and blue fluorophore reporters, since their excitation-emission spectrum is close by, there are chances of bleed through of the signal across channels. To verify if the signal in the blue channel observed while imaging was as a result of bleed through of diffusible GFP reporter expression, TRN::TagBFP:*mak-2[+]* in TRN::GFP background strain was outcrossed with N2 strain (wild type) to remove the integrated diffusible GFP reporter labelling the PLM neuron. The obtained F1 progeny were heterozygous for the marker (lighter GFP expression). The F2 progeny selected were void of the GFP marker. It was verified (Figure 4.1 H) that the signal observed in the blue channel was that of TagBFP::*mak-2* expression and not as a result of bleed through of the diffusible GFP reporter.

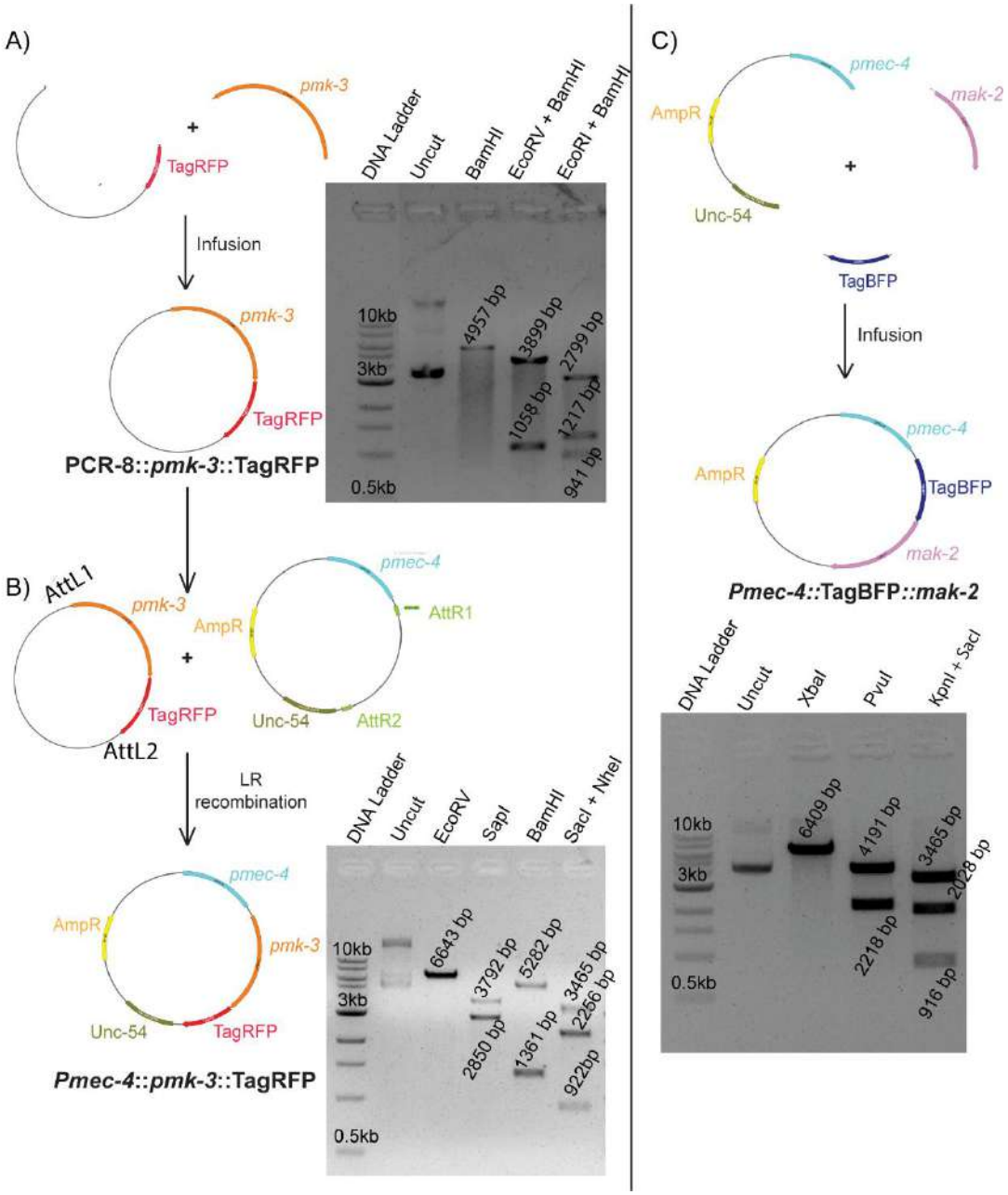
A)
pmk-3
TagRFP
Infusion
pmk-3
TagRFP
PCR-8::pmk-3::TagRFP
DNA Ladder
Uncut
BamHI
EcoRV + BamHI
EcoRI + BamHI
10kb
3kb
0.5kb
4957 bp
3899 bp
2799 bp
1058 bp
1217 bp
941 bp
B)
AttL1
pmk-3
TagRFP
AttL2
pmec-4
AmpR
AttR1
Unc-54
AttR2
LR recombination
pmec-4
AmpR
pmk-3
Unc-54
TagRFP
Pmec-4::pmk-3::TagRFP
DNA Ladder
Uncut
EcoRV
SapI
BamHI
SacI + NheI
10kb
3kb
0.5kb
6643 bp
3792 bp
5282 bp
2850 bp
1361 bp
3465 bp
2256 bp
922bp
C)
pmec-4
mak-2
AmpR
Unc-54
TagBFP
Infusion
pmec-4
AmpR
TagBFP
mak-2
Pmec-4::TagBFP::mak-2
DNA Ladder
Uncut
XbaI
PvuI
KpnI + SacI
10kb
3kb
0.5kb
6409 bp
4191 bp
2218 bp
3465 bp
2028 bp
916 bp

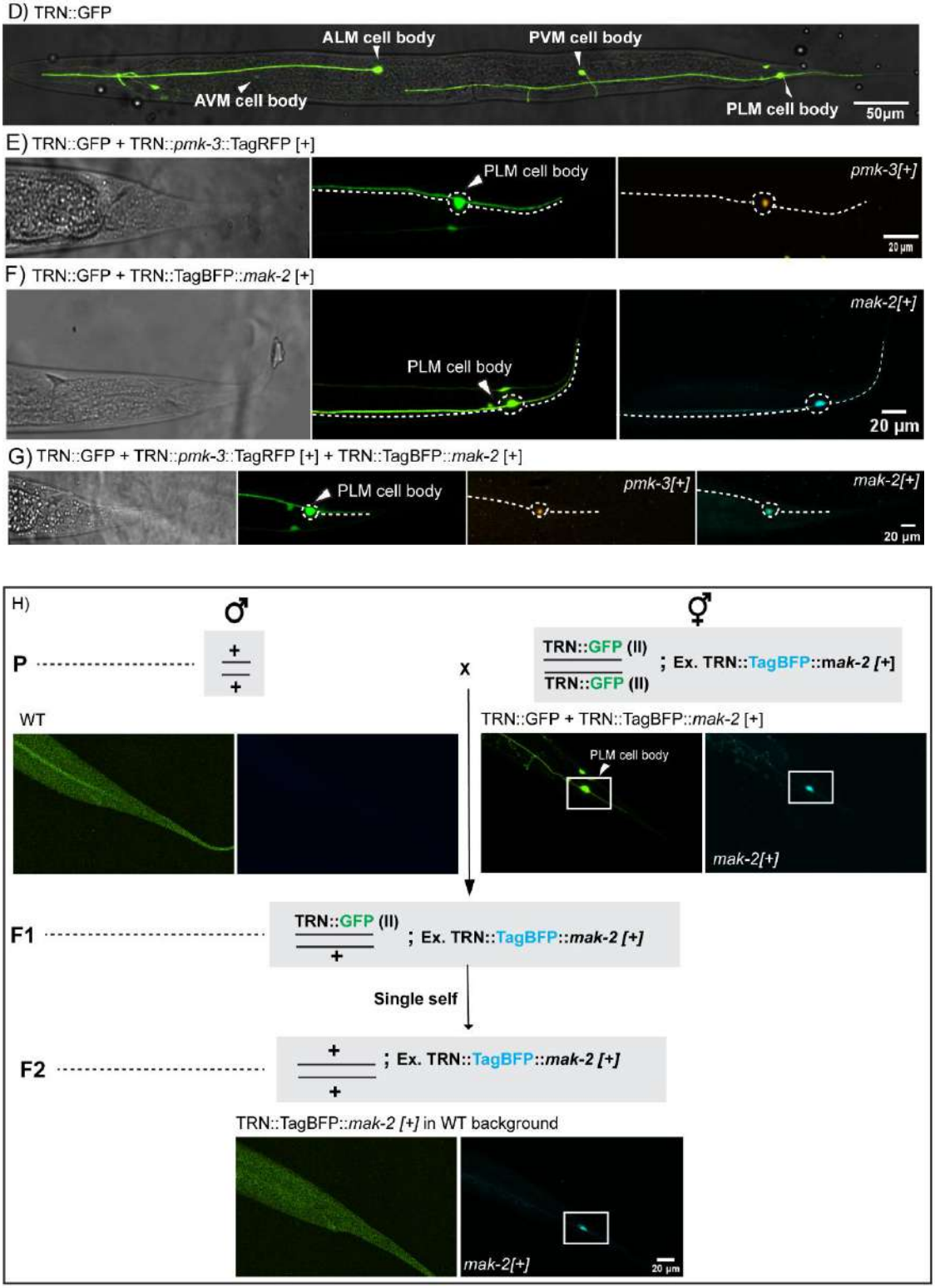

Figure 4.1: Generation of *C. elegans* strains overexpressing PMK-3 and MAK-2

(A-C) Preparation of DNA constructs of PCR-8::*pmk-3*::TagRFP, *Pmec-4*::*pmk-3*::TagRFP and *Pmec-4*::TagBFP::*mak-2* by molecular cloning. *Pmec-4* promoter labelling hereafter has been changed to touch-receptor neuron (TRN) promoter.

(D) Representative confocal image of GFP labelled mechanosensory touch-receptor neuron (TRN) circuit in *C. elegans* (TRN::GFP).

(E-G) Overexpression of *pmk-3* and *mak-2* is denoted by *pmk-3[+]* and *mak-2[+]*. Confocal images representing the expression of *pmk-3[+]*, *mak-2[+]* and *pmk-3[+]*:*mak-2[+]*::1:1 in the TRN::GFP background strains in the PLM mechanosensory neuron

(H) TagBFP::*mak-2* expression was verified by outcrossing the *mak-2[+]* strain with the wild type animal

4.2) Phenotypic characterization of the touch-neuronal circuit due to PMK-3 and MAK-2 overexpression

To evaluate if the overexpression of PMK-3 and MAK-2 causes any morphological changes to the touch-receptor neuronal circuit, phenotypic observations of all the 6 mechanosensory neurons were made and compared to that of the wild type animal (Figure 4.2 A-C). These observations were noted on the mec scoring sheet. It was observed that there were no major cell body positional and morphological changes. The % of animals showing that the PLM anterior process crosses the ALM cell body (Figure 4.2 A) were not significantly different from wild type animals. The ALM posterior process (Figure 4.2 B) is absent in significant number of animals with *pmk-3[+]* and *mak-2[+]* expression compared to that of wild type. Interestingly, when *pmk-3[+]* and *mak-2[+]* are co-expressed in the 1:1 ratio, the presence of ALM posterior process does not seem to be different from that of the wild type animal. All the overexpression strains seem to have a significantly higher occurrence of longer PLM posterior process compared to that of wild type animal (Figure 4.2 C).

Length measurements of the PLM posterior process were performed to complement the phenotyping analysis. Upon *mak-2[+]*, the mean length of PLM posterior process is lesser than that of the wild type animal (Figure 4.2 D). The phenotyping of the overexpression strains provided information about the frequency of occurrence of an observation while the length measurement provided an empirical proof of the observation itself.

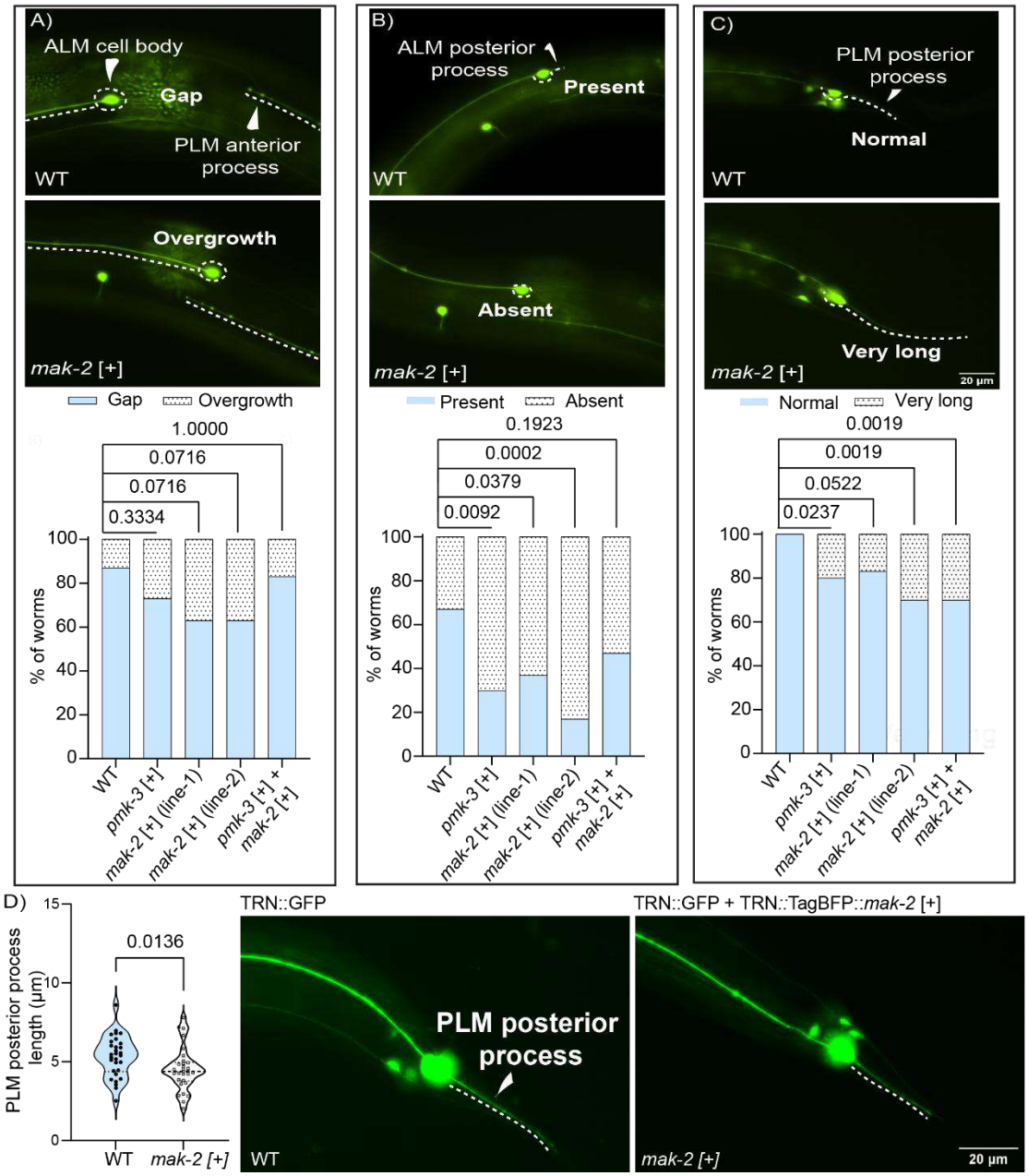

Figure 4.2: Morphological changes in the touch-receptor neuron circuit due to PMK-3 and MAK-2 overexpression

(A – C) Phenotypic characterization of the circuit. Representative images (top) obtained by epifluorescence microscopy of wild type and *mak-2[+]*. All other overexpression strains show similar phenotype as representative images of *mak-2[+]* strain. Contingency plots (bottom) were generated for all the strains in evaluation. Fisher's exact test, two tailed, was applied (N=3, n=30).

(D) The length of PLM posterior process was normalized to the length of the PLM cell body for each worm. This comparison was made across *mak-2[+]* and wild type animal. Man Whitney U test was applied (N=3, n=30).

4.3) PMK-3 and MAK-2 co-expression does not cause puncta formation in the PLM cell body

To evaluate if the overexpression of PMK-3 and MAK-2 can form biomolecular condensates, the strain containing co-expression of *pmk-3 [+]*: *mak-2 [+]* in the TRN::GFP background was used. The PLM cell body of the L4 stage worm was visualized using confocal microscopy (Figure 4.3 A). It was noted that *pmk-3[+]* expression was heavily concentrated within the nucleus of the PLM cell body while *mak-2[+]* was present in both the nucleus and cytoplasm (Figure 4.3 C). This observation was consistent with previous literature (Nakata, Abrams et al. 2005, Yan, Wu et al. 2009). This expression pattern was absent in the wild type animal (TRN::GFP) as expected (Figure 4.3 B). It was noted that, there was no visibility of PMK-3 or MAK-2 puncta within the PLM cell body.

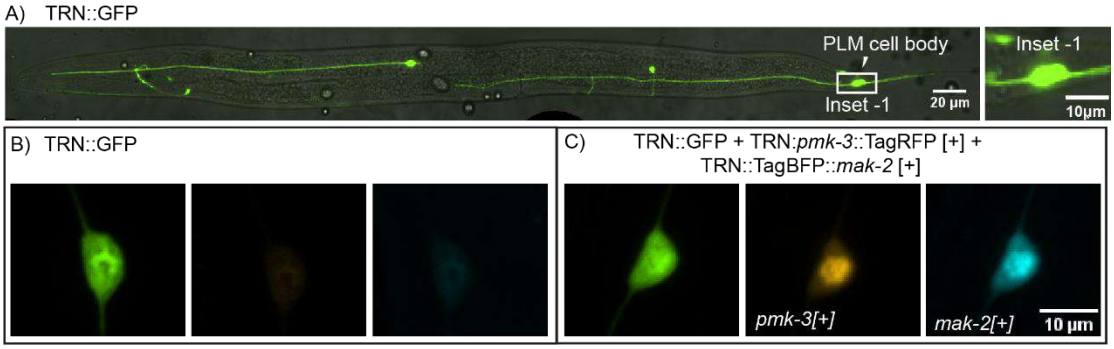

Figure 4.3: *pmk-3[+]* and *mak-2[+]* co-expression does not cause puncta formation in the PLM cell body at L4 stage

(A)Representative confocal image of the touch-receptor neuron circuit highlight the PLM cell body

(B-C) PLM cell body visualized in the green, red and blue channel to see the expression pattern of *pmk-3[+]* and *mak-2[+]* co-expression ((C), N=2, n=12) and compare it with the wild type animal ((B), N=2, n=22).

4.4) Increase in MAK-2 overexpression does not cause puncta formation in the PLM cell body

A recent in-vitro study suggests (Ray, Rao et al. 2024) that, upon increasing MAK-2 concentrations by a few folds than that of PMK-3 can promote/enhance the puncta formation. To evaluate if this observation occurs in in-vivo, a strain containing 1:6::*pmk-3[+]*:*mak-2 [++]* in TRN::GFP background was generated (credits: Chakshu Mangal). The expression of *pmk-3[+]* and *mak-2[++]* in the PLM cell body is as in figure 4.4A.

To check if the increase in *mak-2[++]* expression has any effect on the touch-neuronal circuit, phenotypic observations of the touch-receptor neuron circuit at the L4 stage were made (similar to as mentioned in section 4.2). It was noted that the frequency of PLM anterior process crossing the ALM cell body and the absence of ALM posterior process in the *mak-2[++]* was comparable to that of the wild type animals Figure 4.4 B-C). The occurrence of longer PLM posterior process in the *mak-2[++]* was significantly higher than that of the wild type animals (Figure 4.4 D). Upon evaluating the PLM cell body at the L4 stage, it was observed that the localization of PMK-3 and MAK-2 in the *pmk-3[+]::mak-2[++]* was comparable to that of *pmk-3[+]::mak-2[+]*. It was noted that, *pmk-3[+]::mak-2[++]* has no effect on PMK-3 and MAK-2 puncta formation in the PLM cell body at the L4 stage of the animal.

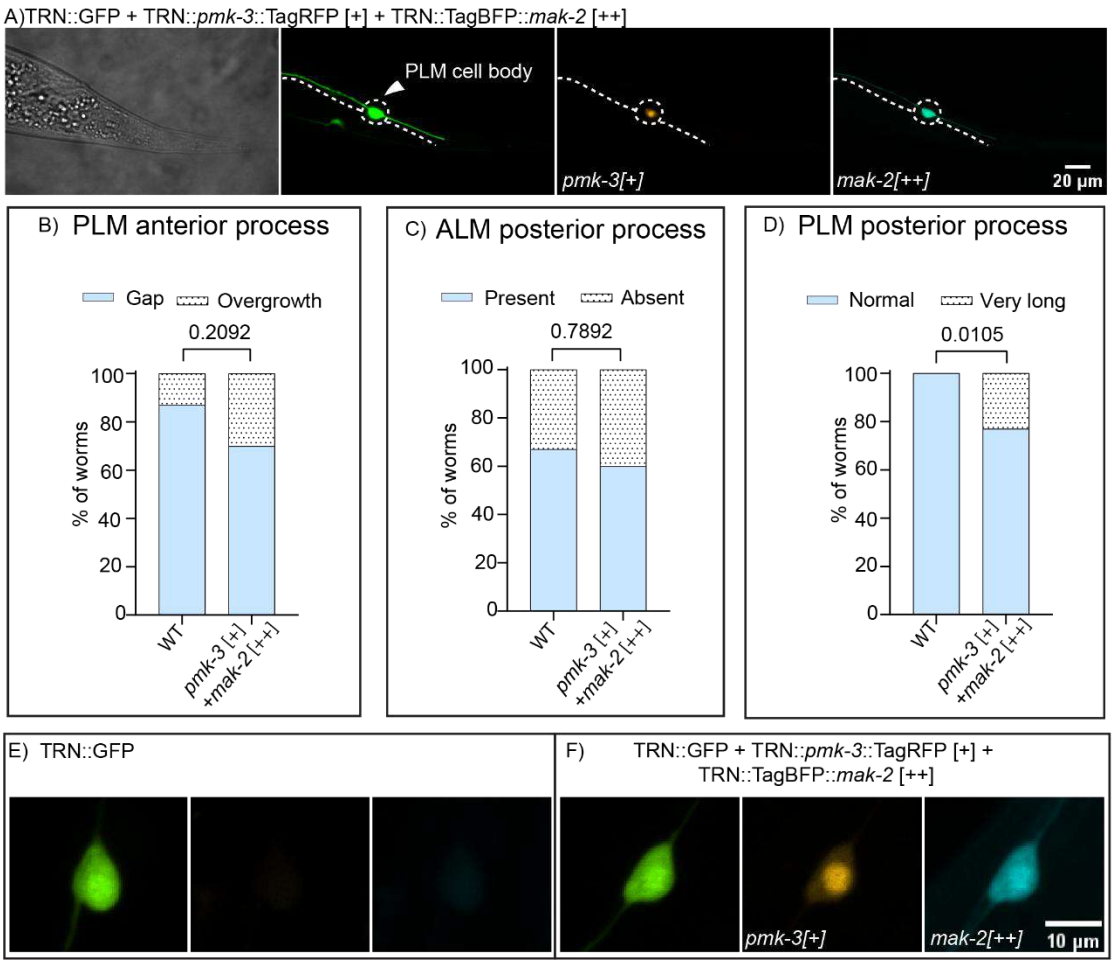

Figure 4.4: *pmk-3[+]* and *mak-2[++]* co-expression does not cause puncta formation in the PLM cell body at L4 stage

(A)Representative confocal image of the expression of *pmk-3[+]::mak-2[++]* in TRN::GFP background in the PLM cell body

(B-D) Phenotypic evaluation of PLM anterior, ALM posterior and PLM posterior process of the *pmk-3[+]::mak-2[++]* in TRN::GFP background strain, Fisher's exact test, two tailed was applied (N=3, n=30).
(E-F) PLM cell body visualized in the green, red and blue channel to see the expression pattern of *pmk-3[+]* and *mak-2[++]* co-expression ((C), N=2, n=14) and compared it with the wild type animal ((B), N=2, n=22).

4.5) PLM Axotomy at L4 stage induces PMK-3 and MAK-2 puncta formation

Despite increasing the concentration of *mak-2[++],* PMK-3 and MAK-2 did not form puncta in the PLM cell body in the regular developing condition of L4 stage. Since the DLK pathway is involved in the axon regeneration response, it was expected that its downstream kinases such as PMK-3 and MAK-2 would be enhanced post axotomy causing formation of puncta. To investigate further, laser-mediated axotomy was performed on the PLM anterior process of the L4 stage of the animal, 50 µm away from the PLM cell body (Figure 4.5A). It is known from previous literature (Tedeschi and Bradke 2013, Basu, Dey et al. 2017) that the DLK pathway is responsible for early regeneration response such as initiation of growth cone formation that occurs approximately at 3 hours post axotomy in *C.elegans* mechanosensory neuron. To aid this response, it was hypothesized for the DLK pathway downstream kinases, PMK-3 and MAK-2 to play an active role during this period. We wanted to see if these kinases can form puncta in-vivo. To study this phenomenon, the PLM cell body was imaged 15 minutes and 3 hours post injury. Axotomy was performed on both strains, overexpressing *pmk-3[+]:mak-2[+]* and *pmk-3[+]:mak-2[++]* also to evaluate, if increase in *mak-2[++],* promotes puncta formation.

As shown in figure 4.5 (B-C), PMK-3 and MAK-2 puncta was observed in the PLM cell body, 15 minutes and 3 hours post axotomy in the L4 stage animals. These puncta were characterized by visual inspection. Local increase in fluorescence intensity of *pmk-3::*TagRFP and TagBFP::*mak-2* in the cytoplasm of the PLM cell body was considered as a puncta. Every puncta that was present in the same spatial location in both the red and blue channel was considered as a single puncta and was accounted for. Each of these puncta were observed in multiple subsequent z-slices (spaced 0.5µm apart), shedding light on its volume. The 2D area of the puncta was measured using ImageJ software, and it ranged between 1.2 μm^2 to 2.1 μm^2. The observed puncta were spatially located at the top or bottom of the cell, as indicated by the slice numbers. Post axotomy (15 minutes and 3 hours), in *pmk-3[+]:mak-2[+]* and *pmk-*

3[+]:mak-2[++] strains, the number of puncta per cell body was plotted (Figure 4.5 B-C).

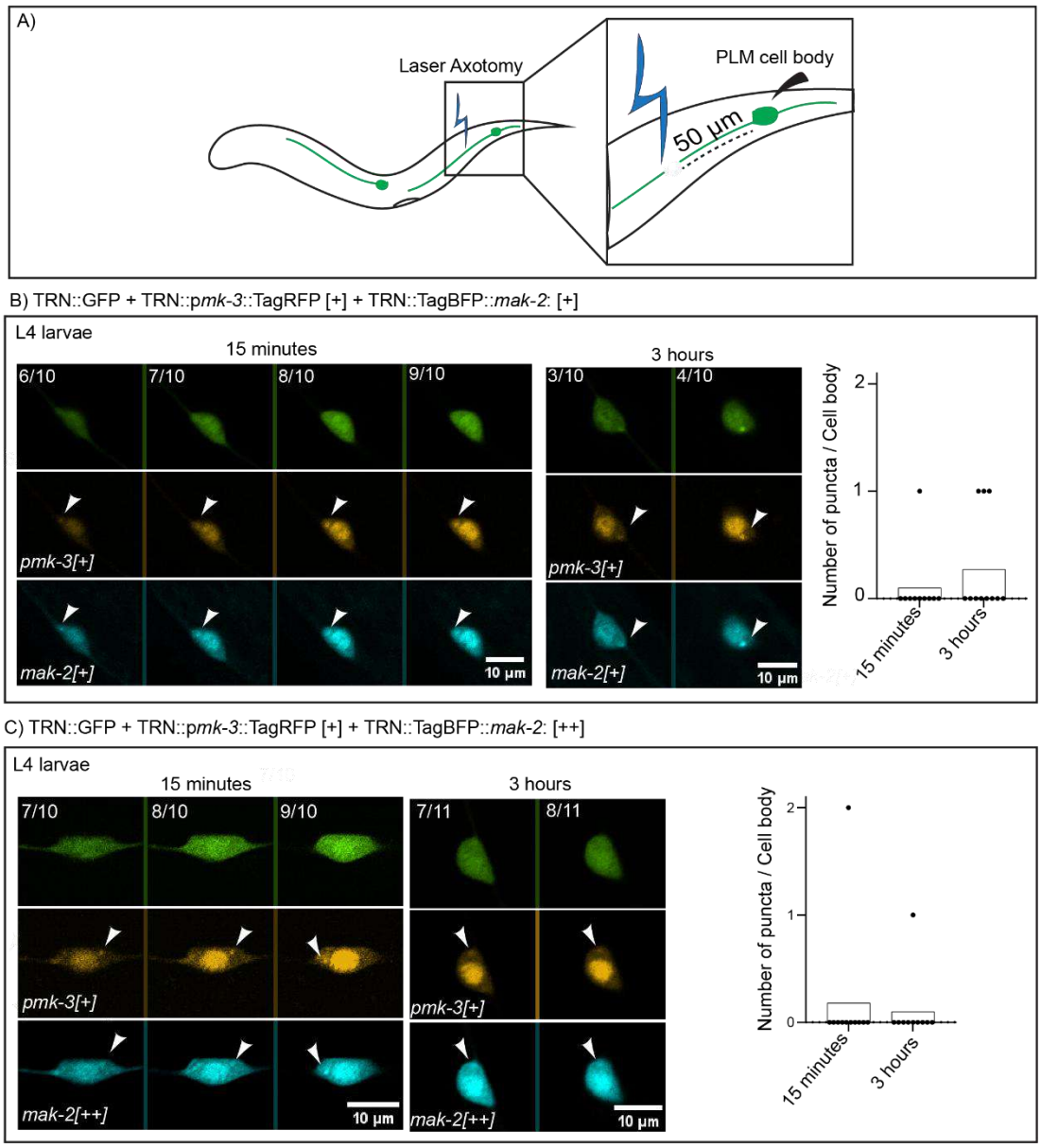

Figure 4.5: Axotomy induced PMK-3 and MAK-2 puncta formation in L4 stage

(A)Diagrammatic representation of site of axotomy on the PLM mechanosensory neuron Number of puncta / cell body was plotted as observed, 15 minutes and 3 hours after axotomy. Each dot, indicates a single PLM cell body, Mean box plot was used for representation. Each z-slice showing puncta is stitched together as a montage and the slice number is labelled on the top left corner. Puncta observed in each slice is indicated by a white arrow head. (B) *pmk-3[+]:mak-2[+]* L4 stage -15minutes (N=2, n=10), 3 hours (N=2, n= 11). (C) *pmk-3[+]:mak-2[++]* L4 stage – 15 minutes (N=2, n=11), 3 hours (N=2, n = 10).

4.6) PMK-3 and MAK-2 puncta increases in size upon axotomy on day 1 and day 3 adults

For us to validate if, the observed puncta at the L4 stage post axotomy was a biomolecular condensate, Fluorescent Recovery After Photo bleaching (FRAP) needs to be performed. But the puncta that was previously observed at both the overexpression strains and time points were smaller in size and poses technical limitations to proceed further. We wanted to see if axotomy in adult animals causes increase in size of formed puncta. Axotomy was performed on day 1 and day 3 adult animals of *pmk-3[+]:mak-2[+]* and *pmk-3[+]:mak-2[++]* strains and the PLM cell body was observed 15 minutes and 3 hours post injury. The 2D area of the PMK-3 and MAK-2 puncta ranges from 0.24µm^2 to 0.47 µm^2. The 3D volume of these puncta is comparable to those observed at L4 stage. The number of puncta per cell body was quantified (Figure 4.6 A-D).

A) TRN::GFP + TRN::p*mk-3*::TagRFP [+] + TRN::TagBFP::*mak-2*: [+]

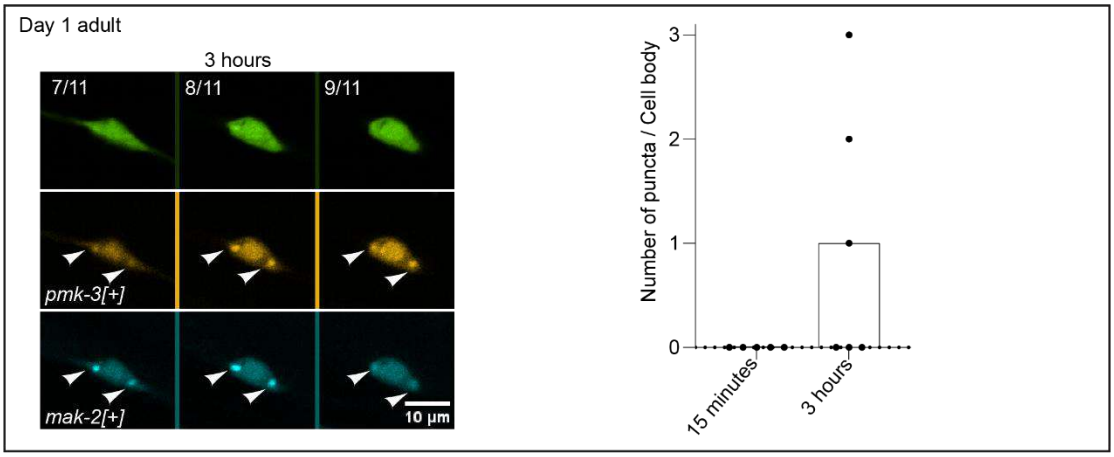

B) TRN::GFP + TRN::p*mk-3*::TagRFP [+] + TRN::TagBFP::*mak-2*: [++]

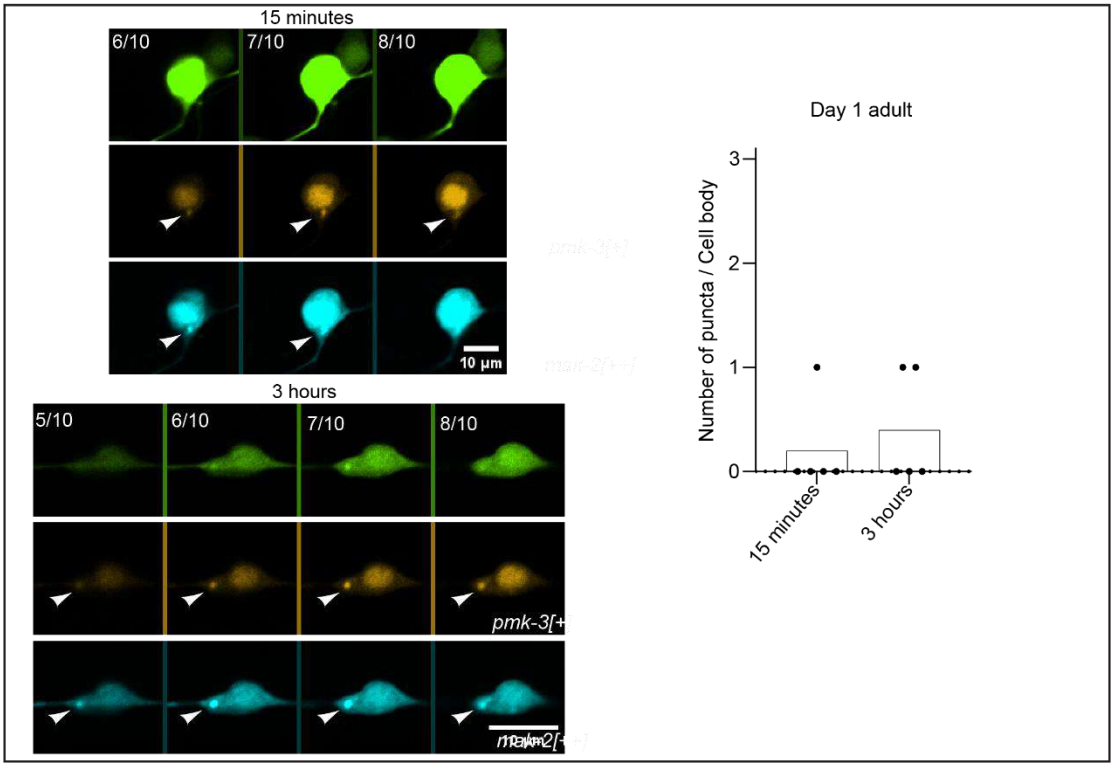

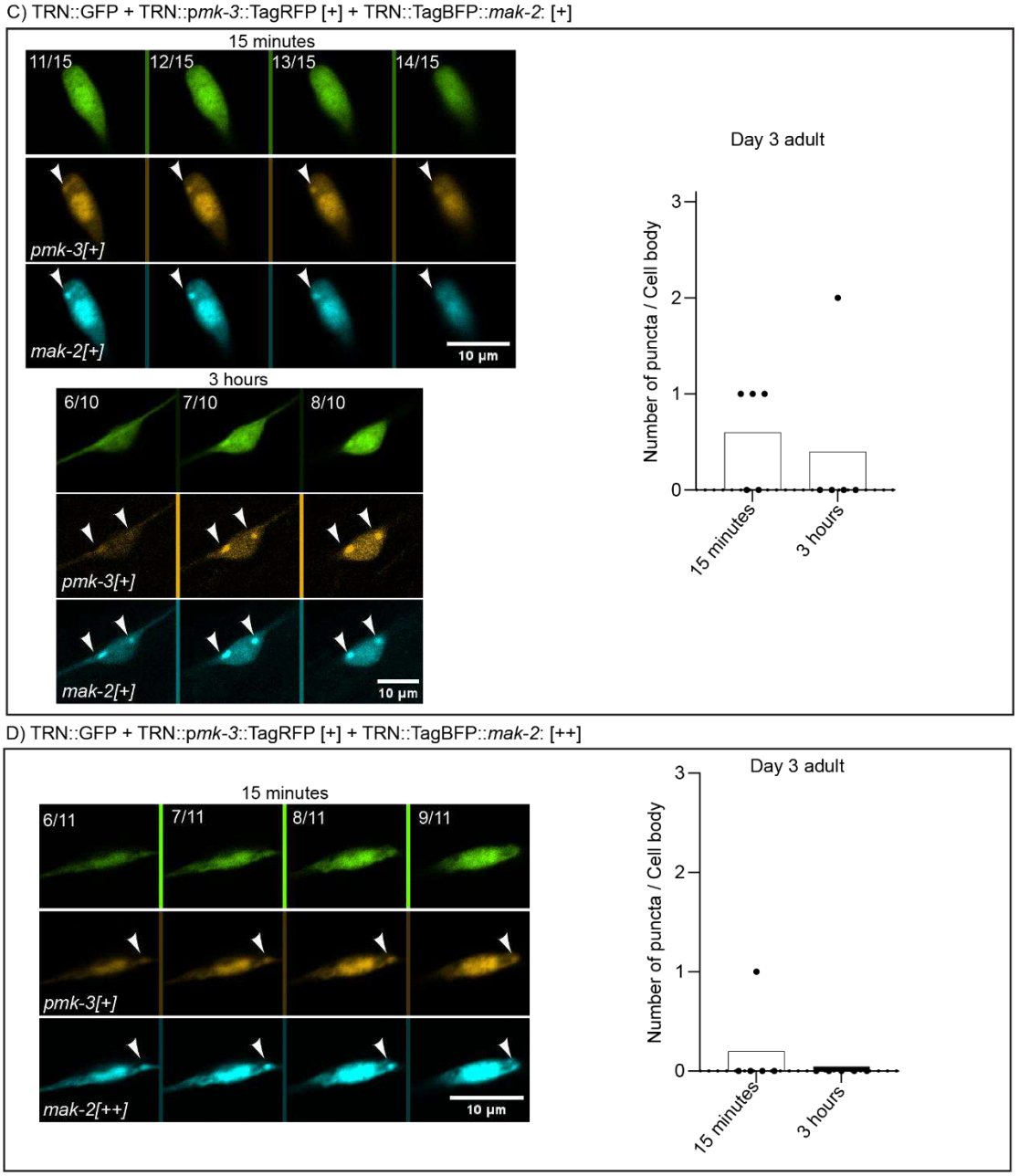

Figure 4.6: PMK-3 and MAK-2 puncta size increases upon axotomy performed on day 1 and day 3 adults

Number of puncta / cell body was plotted as observed, 15 minutes and 3 hours after axotomy on day 1 and day 3 adults. Each dot, indicates a single PLM cell body, Mean box plot was used for representation. Each z-slice showing puncta is stitched together as a montage and the slice number is labelled on the top left corner. Puncta observed in each slice is indicated by a white arrow head. (A) *pmk-3[+]:mak-2[+]* day 1 adult – 15minutes (N=1, n=5), 3 hours (N=1, n= 6). (B) *pmk-3[+]:mak-2[++]* day 1 adult – 15 minutes (N=1, n=5), 3 hours (N=1, n = 5), (C) *pmk-3[+]:mak-2[+]* day 3 adult – 15minutes (N=1, n=5), 3 hours (N=1, n= 6). (D) *pmk-3[+]:mak-2[++]* day 3 adult – 15 minutes (N=1, n=5), 3 hours (N=1, n = 5).

4.7) Preparation of DNA constructs for negative control and overexpression in different tissue

To verify if the PMK-3 and MAK-2 puncta that we see (as mentioned in results 5 and 6) is formed due to *pmk-3::*TagRFP and TagBFP::*mak-2* expression and not solely due to the TagRFP and TagBFP reporters itself, a DNA construct expressing TagBFP under the touch-receptor neuron promoter was prepared (Figure 4.7A).

The PMK-3 and MAK-2 overexpression experiments performed so far (section 4.2 to 4.6), have been in the PLM mechanosensory neuron of the touch-receptor neuron circuit. As relevant it is to study the ability of PMK-3 and MAK-2 to form puncta in the context of axon regeneration in that circuit, it should also be noted that the PLM neuron is small in size. Implying that the scope of visualizing the puncta formation events is lesser relative to a bigger tissue. To increase our ability to capture these events, we aim to investigate the ability of PMK-3 and MAK-2 to form puncta in a different tissue which is relevant to the DLK pathway. For this purpose, a DNA construct expressing *pmk-3::*TagRFP under the *dlk-1* endogenous promoter was prepared (Figure 4.7B).

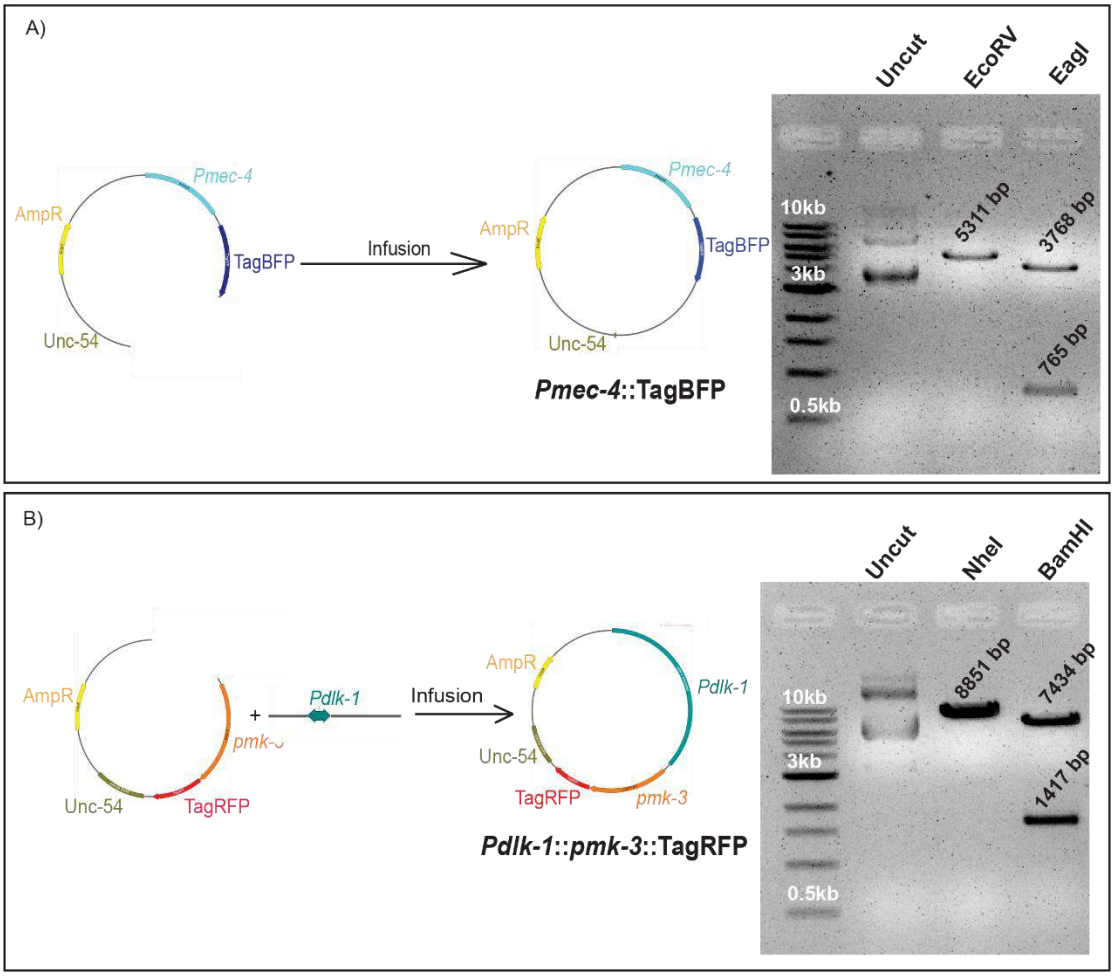

Figure 4.7: Preparation of DNA constructs for *dlk-1* endogenous expression of *pmk-3* and negative control

By molecular cloning, preparation of (A)*Pmec-4::*TagBFP and (B) *Pdlk-1::pmk-3::*TagRFP, where *pmk-3::*TagRFP is expressed in the *dlk-1* endogenous promoter.

5) Discussion

Axons are cellular structures that enable communication across neurons and other tissues. Upon trauma, these structures are damaged and can lead to functional defects. Hence, developing strategies for therapeutic interventions to aid axon regeneration is essential. To do so, understanding the cellular mechanisms involved become crucial. The DLK/p38 MAP kinase pathway is one of the important and evolutionarily conserved pathways responsible for axon regeneration. One of the important questions in the field that remain unanswered is, how is DLK pathway spatially regulated as a response to cellular stress. Theoretical structural analysis of each of the DLK pathway kinases suggest the presence of an intrinsically disordered domain (IDR) indicating their ability to undergo biomolecular condensate formation. A recent *in-vitro* study (Ray, Rao et al. 2024) suggest that, the downstream kinase of the DLK pathway, PMK-3 on its own has the tendency to form aggregates but in the presence of MAK-2 undergo liquid-liquid phase separation (LLPS) and form biomolecular condensates. They further suggest that, this phenomenon might have an implication in increasing the bioavailability of these kinases contributing towards robust functioning of the DLK pathway.

We hypothesized that, PMK-3 and MAK-2 can undergo LLPS-mediated biomolecular condensate formation *in-vivo* and it can play a role in aiding the axon regeneration response. To study this phenomenon, we employed the touch-receptor neuron (TRN) circuit of *C. elegans*, as our model system. This system consists of six mechanosensory neurons namely – 2 ALM, 2 PLM, 1 AVM, 1PVM neurons. PMK-3 and MAK-2 overexpression strains were generated and used for this study. The morphological changes in the TRN circuit caused due to the overexpression was evaluated by phenotyping analysis. Previous literature (Chen, Lee et al. 2014) suggests that overexpression of *dlk*-1 causes a strong PLM axon (anterior process) extension phenotype that can cross the ALM and AVM cell body. Interestingly in our study, overexpression of the DLK-1 downstream kinases such as *pmk-3[+], mak-2[+], pmk-3[+] and mak-2[+],* and *pmk-3[+] and mak-2[++],* showed a neurite tiling phenotype (PLM neurite stops before ALM cell body) which was comparable to that of wild type. This might indicate that overexpression of DLK-1 can causes ectopic neurite growth during development, but the downstream kinases PMK-3 and MAK-2 may not contribute towards it. The ALM posterior process is known to become shorter when DLK-1 was overexpressed in the wild type background (Zheng, Atlas et al. 2020). We observe that, the ALM posterior process is absent in significant number of animals with

pmk-3[+] and *mak-2[+].* Upon co-overexpression of these kinases as in *pmk-3[+]* and *mak-2[+]* and *pmk-3[+]* and *mak-2[++],* the phenotype was comparable to wild type animal. The PLM posterior process is also known to become shorter upon DLK-1 overexpression (Zheng, Atlas et al. 2020). Our observation suggests that, significant number of animals with *mak-2[+],* have a shorter PLM posterior process compared to the wild type animal.

In order to evaluate if PMK-3 and MAK-2 form puncta *in-vivo* at a single cell level, the PLM cell body was observed in the *pmk-3[+]* and *mak-2[+]* of L4 stage of the animal. Upon seeing no puncta, the concentration of *mak-2* was increased (*pmk-3[+]* and *mak-2[++]* as suggested by a previous study (Ray, Rao et al. 2024) to have known to promote puncta formation. We did not observe any puncta formation under this condition.

Since these are downstream kinases of the DLK pathway, responsible for axon regeneration, we hypothesized that, PMK-3 and MAK-2 may form puncta as a response to axotomy. To study further, axotomy was performed on the PLM axon of the L4 stage animals to see if *pmk-3[+]* and *mak-2[+]* and (*pmk-3[+]* and *mak-2[++]* causes puncta formation. It is known from previous literature (Tedeschi and Bradke 2013) that DLK pathway is an early response pathway to injury and is responsible for growth cone initiation. Hence, we hypothesized to see enhancement of its downstream kinases causing puncta formation of PMK-3 and MAK-2 immediately and 3 hours post injury. We observed puncta in the cytoplasm of the PLM cell body with 2D area ranging between 1.2 μm^2 to 2.1 μm^2 and these were observed in the same spatial location across multiple z-slices (0.5 µm apart). In order to evaluate if the puncta formed is a biomolecular condensate, Fluorescent Recovery After Photo bleaching (FRAP) needs to be performed. Since, the PMK-3 and MAK-2 puncta formed after PLM axotomy is smaller, it is technically challenging to perform FRAP on these puncta. Hence, we wanted to see, if the puncta size increases when axotomy was done in day 1 and day 3 adults and validate it further. Upon performing axotomy in *C. elegans* adults, we see an increase in 2D area of the puncta compared to those in L4 stage, and these range from 0.24μm^2 to 0.47 μm^2. The 3D size of these puncta was comparable to that during L4, characterized by the number of z-slices the puncta is spanning. Since all of these experiments are done with *C. elegans* strains expressing extrachromosomal array, the amount of expression of these proteins (tagged with translational reporters) in question vary across animals. Hence, fluorescence intensity measurements for puncta characterization might not be a good measure. But this system is an excellent tool to

evaluate the penetrance of the phenotype in question. So far, all the observations regarding PMK-3 and MAK-2 puncta in the PLM cell body is noted, however, the number of biological replicates and sample size of the experiment should be increased in order to make any statistically significant conclusions.

6) Future prospects

- The sample number and biological replicates for L4, day 1 and day 3 stage PLM axotomy experiments to visualize PMK-3 and MAK-2 puncta must be increased to evaluate the penetrance of the phenotype.
- The PLM cell body of day 1 and day 3 staged animals without axotomy must be visualized to see if the PMK-3 and MAK-2 puncta formed is due to axotomy or if aging plays a role.
- To verify that the PMK-3 and MAK-2 puncta visualized in the red and blue channel is due to the expression of *pmk-3::*TagRFP and TagBFP::*mak-2,* negative control experiments with the same experimental paradigm must with conducted with TRN::TagBFP and TRN::TagRFP overexpression strains.
- To validate if the PMK-3 and MAK-3 puncta observed is a biomolecular condensate, Fluorescent Recovery After Photo bleaching (FRAP) on the puncta needs to be performed. Due to the dynamical state of the condensate, fluorescence recovery is expected to occur. Biomolecular condensates can also be tested by live imaging of the PLM cell body to visualize the fusion and fission of puncta.
- To further validate, if MAK-2 is the driver of PMK-3 and MAK-2 biomolecular condensate formation, axotomy experiments can be performed in the strain containing PMK-3 overexpression in the *mak-2(ok2394)* mutant background, expecting to see no puncta formation.
- To study PMK-3 and MAK-2 puncta formation in a bigger tissue to increase the chances of visualizing these events, its expression can be studied by overexpressing them under the *dlk-1* promoter.

7) References

Albeg, A., C. J. Smith, M. Chatzigeorgiou, D. G. Feitelson, D. H. Hall, W. R. Schafer, D. M. Miller, 3rd and M. Treinin (2011). "C. elegans multi-dendritic sensory neurons: morphology and function." Mol Cell Neurosci **46**(1): 308-317.

Andrusiak, M. G., P. Sharifnia, X. Lyu, Z. Wang, A. M. Dickey, Z. Wu, A. D. Chisholm and Y. Jin (2019). "Inhibition of Axon Regeneration by Liquid-like TIAR-2 Granules." Neuron **104**(2): 290-304 e298.

Apweiler, R., A. Bairoch, C. H. Wu, W. C. Barker, B. Boeckmann, S. Ferro, E. Gasteiger, H. Huang, R. Lopez, M. Magrane, M. J. Martin, D. A. Natale, C. O'Donovan, N. Redaschi and L. S. Yeh (2004). "UniProt: the Universal Protein knowledgebase." Nucleic Acids Res **32**(Database issue): D115-119.

Basu, A., S. Dey, D. Puri, N. Das Saha, V. Sabharwal, P. Thyagarajan, P. Srivastava, S. P. Koushika and A. Ghosh-Roy (2017). "let-7 miRNA controls CED-7 homotypic adhesion and EFF-1-mediated axonal self-fusion to restore touch sensation following injury." Proc Natl Acad Sci U S A **114**(47): E10206-E10215.

Boulin, T., J. F. Etchberger and O. Hobert (2006). "Reporter gene fusions." WormBook: 1-23.

Brenner, S. (1974). "The genetics of Caenorhabditis elegans." Genetics **77**(1): 71-94.

Chen, C. H., A. Lee, C. P. Liao, Y. W. Liu and C. L. Pan (2014). "RHGF-1/PDZ-RhoGEF and retrograde DLK-1 signaling drive neuronal remodeling on microtubule disassembly." Proc Natl Acad Sci U S A **111**(46): 16568-16573.

Chen, L. and A. D. Chisholm (2011). "Axon regeneration mechanisms: insights from C. elegans." Trends Cell Biol **21**(10): 577-584.

Flibotte, S., M. L. Edgley, I. Chaudhry, J. Taylor, S. E. Neil, A. Rogula, R. Zapf, M. Hirst, Y. Butterfield, S. J. Jones, M. A. Marra, R. J. Barstead and D. G. Moerman (2010). "Whole-genome profiling of mutagenesis in Caenorhabditis elegans." Genetics **185**(2): 431-441.

Ganser, L. R. and S. Myong (2020). "Methods to Study Phase-Separated Condensates and the Underlying Molecular Interactions." Trends Biochem Sci **45**(11): 1004-1005.

He, Z. and Y. Jin (2016). "Intrinsic Control of Axon Regeneration." Neuron **90**(3): 437-451.

Hisamoto, N. and K. Matsumoto (2017). "Signal transduction cascades in axon regeneration: insights from C. elegans." Curr Opin Genet Dev **44**: 54-60.

Lambert, T. J. (2019). "FPbase: a community-editable fluorescent protein database." Nat Methods **16**(4): 277-278.

Mello, C. C., J. M. Kramer, D. Stinchcomb and V. Ambros (1991). "Efficient gene transfer in C.elegans: extrachromosomal maintenance and integration of transforming sequences." Embo j **10**(12): 3959-3970.

Nakata, K., B. Abrams, B. Grill, A. Goncharov, X. Huang, A. D. Chisholm and Y. Jin (2005). "Regulation of a DLK-1 and p38 MAP kinase pathway by the ubiquitin ligase RPM-1 is required for presynaptic development." Cell **120**(3): 407-420.

Park, E. C., D. R. Glodowski and C. Rongo (2009). "The ubiquitin ligase RPM-1 and the p38 MAPK PMK-3 regulate AMPA receptor trafficking." PLoS One **4**(1): e4284.

Rao, G. N., S. S. Kulkarni, S. P. Koushika and K. R. Rau (2008). "In vivo nanosecond laser axotomy: cavitation dynamics and vesicle transport." Opt Express **16**(13): 9884-9894.

Ray, P., P. T. Rao, M. Nandi, A. Haque, S. Mitra, S. Raychaudhuri, A. Ghosh-Roy and S. Polley (2024). "Activation and regulation of a p38α MAPK by its downstream MAPKAP kinase through feedback phosphorylation and LLPS-driven condensate formation." bioRxiv: 2024.2008.2001.606155.

Rostam, N., S. Ghosh, C. F. W. Chow, A. Hadarovich, C. Landerer, R. Ghosh, H. Moon, L. Hersemann, D. M. Mitrea, I. A. Klein, A. A. Hyman and A. Toth-Petroczy (2023). "CD-CODE: crowdsourcing condensate database and encyclopedia." Nat Methods **20**(5): 673-676.

Scheib, J. and A. Hoke (2013). "Advances in peripheral nerve regeneration." Nat Rev Neurol **9**(12): 668-676.

Tedeschi, A. and F. Bradke (2013). "The DLK signalling pathway--a double-edged sword in neural development and regeneration." EMBO Rep **14**(7): 605-614.

Varadarajan, S. G., J. L. Hunyara, N. R. Hamilton, A. L. Kolodkin and A. D. Huberman (2022). "Central nervous system regeneration." Cell **185**(1): 77-94.

Wang, B., L. Zhang, T. Dai, Z. Qin, H. Lu, L. Zhang and F. Zhou (2021). "Liquid-liquid phase separation in human health and diseases." Signal Transduct Target Ther **6**(1): 290.

Yan, D., Z. Wu, A. D. Chisholm and Y. Jin (2009). "The DLK-1 kinase promotes mRNA stability and local translation in C. elegans synapses and axon regeneration." Cell **138**(5): 1005-1018.

Zheng, C., E. Atlas, H. M. T. Lee, S. L. J. Jao, K. C. Q. Nguyen, D. H. Hall and M. Chalfie (2020). "Opposing effects of an F-box protein and the HSP90 chaperone network on microtubule stability and neurite growth in Caenorhabditis elegans." Development **147**(12).

8) Appendix

Section -1: Detailed experimental conditions

1) Molecular cloning

1.1)PCR conditions

Vector backbone				
Construct	Vector template	Amplicon	Polymerase	Primers
pNBRGWY188_PCR-8::*pmk-3*::TagRFP	pNBR45_PCR-8::*ptrn-1*::TagRFP	PCR-8::*ptrn-1*::TagRFP sans *ptrn-1*(5221bp)	CloneAmp Hifi PCR polymerase	AGR1374, AGR608
pNBR78_*pmec-4*::TagBFP::*mak-2*	pNBRGWY54_p*mec-4*::mscarlet	pmec-4::mscarlet sans mscarlet (5385 bp)	PrimeStar DNA polymerase	AGR648, AGR649
pNBR79_*pmec-4*::TagBFP	pNBR78_*pmec-4*::TagBFP::*mak-2*	*pmec-4*::TagBFP::*mak-2* sans *mak-2* (5311 bp)	CloneAmp Hifi PCR polymerase	AGR1417, AGR1418
pNBR80_*pdlk-1*::*pmk-3*::TagRFP	pNBRGWY189_*pmec-4*::*pmk-3*::TagRFP	*pmec-4*::*pmk-3*::TagRFP sans p*mec-4* (5621 bp)	PrimeStar DNA polymerase	AGR592, AGR593

Insert				
Construct	Insert template	Amplicon	Polymerase	Primers
pNBRGWY188_PCR-8::*pmk-3*::TagRFP	pNBRGWY28_PCR-8::*pmk-3*	*pmk-3* (1422 bp)	CloneAmp Hifi PCR polymerase	AGR1372, AGR1373
pNBR78_*pmec-4*::TagBFP::*mak-2*	Adgene plasmid # 124343	TagBFP (804 bp)	PrimeStar DNA polymerase	AGR1386, AGR1387
	yk2020f16_Kohara collection - mak-2 c-DNA	*mak-2* (1101 bp)	PrimeStar DNA polymerase	AGR1388, AGR1389
pNBR80_*pdlk-1*::*pmk-3*::TagRFP	Fosmid WRM069cA04 (I)	*pdlk-1* (3230 bp)	Q5 DNA polymerase	AGR1467, AGR1481

1.2)PCR/gel purification/Cloner enhancer

Clone name	**Product**	**Type of purification**
Pmec-4::TagBFP	Linearized *Pmec-4*::TagBFP	Gel extraction
Pdlk-1::*pmk-3*::TagRFP	*Pdlk-1* promoter	PCR purification

Cloner Enhancer	
Clone name	**Product**

PCR-8::*pmk-3*::TagRFP	PCR-8::TagRFP linear, *pmk-3*
Pdlk-1::*pmk-3*::TagRFP	*Pmec-4*::*pmk-3*::TagRFP sans *Pmec-4* - vector backbone
Pmec-4::TagBFP::*mak-2*	*Pmec-4*::mscarlet sans mscarlet, TagBFP, *mak-2*

1.3)Infusion/Gateway cloning

Clone name	Type of cloning	Number of fragments	Ratios (Insert: vector)	Quantity		
				Vector backbone	Insert 1	Insert 2
PCR-8::*pmk-3*::TagRFP	Infusion	2	2:1	19.65ng /	16.84ng /	N/A
Pmec-4::TagBFP::*mak-2*	Infusion	3	2:02:01	8.75 ng /	TagBFP - 3.11 ng	*mak-2* - 4.278 ng
Pmec-4::TagBFP	Site-directed insertion_Infusion	1	N/A	25ng	N/A	N/A
Pdlk-1::*pmk-3*::TagRFP	Infusion	2	2:1	11.42ng / 3.298 fmol	13.12ng / 6.595 fmol	N/A

Clone name	Type of cloning	Destination clone	Entry Clone	Ratio
Pmec-4::*pmk-3*::TagRFP	Gateway	PCZGY553_LR_Pmec-4	PCR-8::*pmk-3*::TagRFP	1:1
		37.5 ng	37.5 ng	

1.4)Colony PCR

Clone name	Strategy	Size of desired bands	Primers		Number of colonies screened	Number of positive colonies obtained
			Forward primer	Reverse primer		
PCR-8::*pmk-3*::TagRFP	PCR-8 vector backbone - *pmk-3* junction	1497 bp	AGR738	AGR1373	16	colony 3
Pmec-4::*pmk-3*::TagRFP	Intronic region on the vector - *pmk-3* junction	1500 bp	AGR415	AGR1373	16	colony 4
Pmec-4::TagBFP::*mak-2*	synthetic intron vector - TagBFP junction	943 bp	AGR415	AGR1387	16	colony 3
	TagBFP-*mak-2* junction	1919 bp	AGR1386	AGR1389		
	mak-2 - vector (unc-54) junction	1285 bp	AGR1388	AGR1073		

Pdlk-1::*pmk-3*::TagRFP	*Pdlk-1* - PCR-8 vector backbone junction	913 bp	AGR1497	AGR649	48	colony 113
Pmec-4::TagBFP	TagBFP- unc-54 vector backbone junction	560 bp	AGR1470	AGR1073	16	colony 13

1.5) Restriction digestion

Clone name	Restriction enzymes	Expected band size
PCR-8::*pmk-3*::TagRFP	BamHI	4957 bp
	EcoRV + BamHI	3899 bp, 1058 bp
	EcoRI + BamHI	2799 bp, 1217 bp, 941 bp
Pmec-4::*pmk-3*::TagRFP	EcoRV	6643 bp
	BamHI	5282 bp, 1361bp
	SacI + NheI	3465 bp, 2256 bp, 922bp
Pmec-4::TagBFP::*mak-2*	XbaI	6409 bp
	PvuI	4191 bp, 2218 bp
	SapI	3792bp, 2850bp
	KpnI + SacI	3465 bp, 2028 bp, 916 bp
Pmec-4::TagBFP	EcoRV	5311 bp
	EagI	3768 bp, 765 bp
	PvuI + EcoRI	2805 bp, 1706 bp, 822 bp
Pdlk-1::*pmk-3*::TagRFP	NheI	8851 bp
	BamHI	7434 bp, 1417 bp

1.6)Sanger's sequencing

Clone name	Segment sequenced	Primers used
PCR-8::*pmk-3*::TagRFP	pmk-3::TagRFP	AGR738, AGR739, AGR740, AGR741
Pmec-4::*pmk-3*::TagRFP	pmk-3::TagRFP	AGR415, AGR1073, AGR1372, AGR1373, AGR1374, AGR1419, AGR1469
Pmec-4::TagBFP::*mak-2*	TagBFP::mak-2	AGR415, AGR1073, AGR1386, AGR1409, AGR1420, AGR1470
Pmec-4::TagBFP	TagBFP	AGR415, AGR1073, AGR1386, AGR1470
Pdlk-1::*pmk-3*::TagRFP	*Pdlk-1* region	AGR1467, AGR1481, AGR1497

2)Genotyping

To validate if the co-localized PMK-3 and MAK-2 puncta formation was as a result of their functional interaction, protein loss of function mutant strains were obtained. These mutants were first verified by genotyping. The external forward and reverse primers were designed to bind outside the mutation region, whereas internal forward primers were bound to the gene sequence. The band sizes of external forward + reverse primers of mutants should be shorter as compared to the N2 / wildtype strain. Whereas, the internal forward + reverse primers of mutants should yield no band. The genomic DNA was obtained from gravid adults containing eggs.

	Primers		
Strain details	**External forward**	**Internal Forward**	**Reverse**
pmk-3(ok169) IV	AGR193	AGR194	AGR195
mkk-4(ok1545)	AGR1412	AGR1413	AGR1414
mak-2(ok2394) IV	AGR1409	AGR1410	AGR1411

Expected bands during Genotyping		
Primers	**N2**	**pmk-3(ok169)**
External forward + Reverse primer	1602 bp	409 bp
Internal forward + Reverse primer	604 bp	No band
Primers	**N2**	**mkk-4(ok1545)**
External forward + Reverse primer	1511 bp	495 bp
Internal forward + Reverse primer	628 bp	No band
Primers	**N2**	**mak-2(ok2394) IV**
External forward + Reverse primer	1230 bp	352 bp
Internal forward + Reverse primer	843 bp	No band

PCR conditions:

	pmk-3 (ok169)			
Initial Denaturation	**Denaturation**	**Annealing**	**Extension**	**Final Extension**
98 °C	98 °C	64 °C	72 °C	72 °C
2 minutes	10 seconds	30 seconds	1 minute 40 seconds	10 minutes
1X	35X			1X

	mak-2 (ok2394)			
Initial Denaturation	**Denaturation**	**Annealing**	**Extension**	**Final Extension**

98 °C	98 °C	60 °C	72 °C	72 °C
2 minutes	10 seconds	30 seconds	1 minute 15 seconds	10 minutes
1X	35X			1X

	mkk-4 (ok1545)			
Initial Denaturation	**Denaturation**	**Annealing**	**Extension**	**Final Extension**
98 °C	98 °C	62 °C	72 °C	72 °C
2 minutes	10 seconds	30 seconds	1 minute 15 seconds	10 minutes
1X	35X			1X

Section -2 : Integration of Extrachromosomal array into the genome of *C.elegans*

1) Introduction

The PVD neuron in *Caenorhabditis elegans* is responsible for mechanosensation, thermosensation and maintains body posture. This neuron has a distinct dendrite and axonal compartments. It has an elaborate dendritic structure that spans the whole-body length of the animal. The primary dendrite that runs at the central body line of the worm. Multiple secondary dendrites are seen arising perpendicular to the primary dendrite. The tertiary dendrite runs parallel to the primary dendrite and multiple quaternary dendrite are perpendicularly arising from the tertiary. This branching pattern of the dendrite is often compared to that of a Menorah. Because of its elaborate dendritic structure, it serves as a suitable model system to study dendrite regeneration (Albeg, Smith et al. 2011).

In-order to perform dendrotomy, the entire neurite compartment is labelled to express a diffusible fluorescence reporter to aid visualization of the neuron. A transgenic *C. elegans* strain with an extrachromosomal array expression of this reporter would not cause 100% of the progeny to have the marker alongside having non-uniform expression across animals. It also happens that continuous rearing of animals containing the array may eventually cause loss of propagation to its progeny, as they do not follow Mendelian form of inheritance. To overcome these shortcomings, the extrachromosomal array can be integrated into the genome of the worm.

2) Materials and methods

The integration of the extrachromosomal array into the worm's genome (Mello, Kramer et al. 1991) was done by the TMP-UV irradiation method. The wild type animals and extrachromosomal strain *ser2prom3::*mscarlet; *ttx3::*RFP(ShrEx472) were treated in the following way:

a) Preparation of mutagen:

1mg/ml stock of Trimethylpsoralen (TMP), a light-sensitive mutagen, was freshly prepared by weighing 0.001g of TMP and dissolving it in 1ml 100% DMSO. 0.1mg/ml working solution was prepared by mixing 20$\mu\ell$ of 1mg/ml stock of TMP with 180$\mu\ell$ of 1X M9 buffer.

b) Preparation of sample:

95-98 L4 staged worms of strain of interest were obtained and transferred into 200ul of 1X M9 buffer.

c) Treatment of worms with mutagen:

The worm sample prepared was treated with 1:1 (200$\mu\ell$) working solution of TMP and 1X M9 buffer and incubated in the dark for 30 minutes. The treated worms were then transferred onto an unseeded NGM plate and kept in dark.

d) Setting up the collimeter apparatus:

The LED was connected to the collimeter. The collimeter was connected to the regulator and power adapter (1.3W). The collimeter was adjusted to level 5 to ensure coverage of the whole NGM plate and to ensure continuous wave of UV, the controller was set at 50% (78J).

e) UV irradiation:

The plate containing TMP mutagen treated worms was placed below the collimeter in the dark and the complete plate was illuminated with UV at 50% intensity for 1 minute. Further the plate was kept in dark.

f) Preparation of OP50 culture and rescue of treated worms:

15 ml of freshly inoculated B-broth with *E. coli* OP50 strain was centrifuged at 4000 rpm for 15 minutes. The supernatant was decanted and the pellet was resuspended in 1ml B-broth. This culture was added to the treated worms and kept for drying in the dark. The plate was kept at 15ºC overnight and each Po was copied onto a new freshly seeded plate. Each plate was labelled with P_n and date, where n is the parent number, signifying 'n' parent plates.

g) Collection of F1 progeny:

F1's from all the parent plates were individually transferred to a new plate containing the *pser2prom3*::mcherry and *ttx3*::RFP markers and were grown at 20ºC. Each F1 plate was labelled by P_nF1_m, where n is the parent plate number and m is the F1 progeny plate number.

h) Selection of F2 progeny:

The transmission efficiency was calculated for all the F1 plates, and the ones that showed closer to / greater than 75% were selected. 8 F2 worms were individually

transferred to separate plates for further tracking. Each plate was labelled with $P_nF1_mF2_p$, where n, m and p are the parent, F1 and F2 plate numbers respectively.

i) Selection of F3 progeny:

The transmission efficiency was calculated in all the F2 progeny plates. The plates showing 100% transmission of the *ser2prom3::*mscarlet; *ttx3::*RFP(ShrIs4) marker were selected and further propagated.

3) Result

Optimization of the percentage of UV irradiation was done to ensure the TMP-UV irradiation has an impact on the animal (characterized by the sickness of the worm), and yield sufficient survival. For this purpose, the wild type animals were treated with 0.1mg/ml of TMP mutagen and different percentages of UV irradiation as mentioned in table 3.

Percentage (%)	Total number of worms treated	Total survived
0	20	11
25	20	6
50	20	19
80	20	7
100	10	1

Table 3: Wild type animals undergoing TMP-UV mutagenesis

Upon mutagenesis, the animals showed various phenotypes such as slow movement, coiling, sick, dead, flatter sinusoidal movement, leakage of alimentary canal, slender and certain defects such as egg laying defect, egg hatching defect, slower response to gentle touch, paralysis of posterior end of the worm. Some of the phenotypes are depicted in figure 3B.

It was to note that 0.1mg/ml treatment of TMS mutagen along with 50% UV exposure was impactful and yielded maximum survival of animals. This combination of treatment was used on the transgenic strain containing *ser2prom3::*mscarlet; *ttx3::*RFP(ShrEx472). Transgenic line having the extrachromosomal array with low

transmission efficiency were used to cause its integration into the genome. The growing plate of this line before integration is indicated in figure 3A, where the transmission efficiency was 34%. Upon integration of the array, their propagation to their progeny follow Mendelian form of inheritance (Figure 3D). A growing plate with an integrant line has 100% transmission to their progeny (Figure 3C). The expression of the integrated array was visualized in the PVD neuron at a higher magnification (Figure 3E).

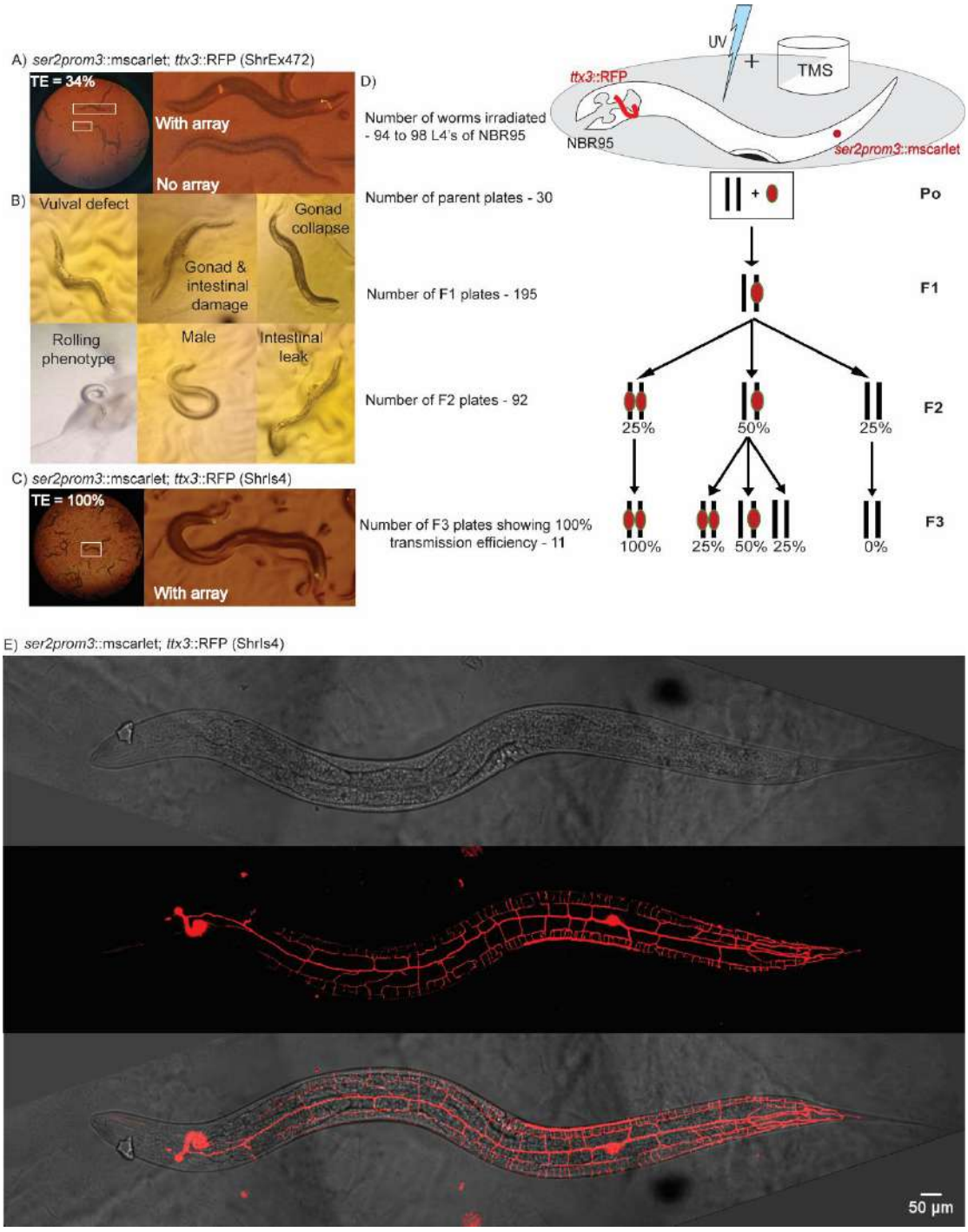

Figure 3: Integration of extrachromosomal array by the TMP-UV irradiation method

(A)Representative image of a growing plate of animals containing the extrachromosomal array of *ser2prom3::*mscarlet; *ttx3::*RFP(ShrEx472)

(B)Representative images of various defects caused by TMP-UV irradiation in *C.elegans.*

(C)Integrated extrachromosomal array follows Mendelian form of inheritance

(D)Representative image of a growing plate containing animals with 100% transmission efficiency, *ser2prom3::*mscarlet; *ttx3::*RFP(ShrIs4)

(E)Representative Confocal image of the integrated line showing diffusible mscarlet expression in the PVD neuron in *ser2prom3::*mscarlet; *ttx3::*RFP(ShrIs4). DIC image (Top), Red channel (middle), merged (bottom).

Discussion

4,5′,8-trimethylpsoralen (TMP) when combined with near UV light behaves as a mutagen by forming inter-strand DNA crosslinks. It is known to cause small deletions in the genome of *C.elegans* (Flibotte, Edgley et al. 2010). It is expected that the cells while repairing the DNA damage, might integrate the extrachromosomal array into the genome, as a chance event. To increase this probability of integration, a greater number of transgenic animals are treated with the mutagen.

To select the animals across generations, 2 factors were crucial: 1) % transmission efficiency, 2) Intensity of the reporter (of either the co-injection marker or pser2prom-3::mcherry). In the F2 generation, the transmission efficiency observed was between 75 to 100%. Indicating that, these animals could be a homo/heterozygous integrated animal containing a copy of the extrachromosomal array. The intensity of the reporter expression across different lineage animals were different, which might be because of the background mutations present. Hence, it was not a good measure to select animals based on brighter fluorescence. Animals showing 100% transmission of the marker to its progeny were obtained as an integrated line in their F3 stage and were propagated.

Future prospects

The obtained integrant lines should be outcrossed and single-selfed with the wild type males for 5 times to remove the background mutations caused due to the mutagenesis.